

Parameters extraction of single and double diodes photovoltaic models using Marine Predators Algorithm and Lambert W function

Hussein Mohammed Ridha *

*Department of Electrical and Electronics Engineering, Faculty of Engineering, Universiti Putra Malaysia, 43400 Serdang, Malaysia
Advanced Lightning, Power and Energy Research, Faculty of Engineering, Universiti Putra Malaysia, 43400 Serdang, Malaysia*

ARTICLE INFO

Keywords:

Modeling of PV module
Single diode model
Double diode model
Marine Predators Algorithm
Lambert W function

ABSTRACT

Efficient and accurate estimation parameters of the PV model from real experimental data is crucial for modeling, increasing investments, and determining the actual performance before installing the PV panels. Recently, several stochastic methods have been proposed to extract the parameters of the PV module/cells optimally. However, some of these approaches have restrictions in terms of exploration and exploitation capacities individually or combined due to their stochastic searching strategies. In this research work, Marine Predator Algorithm (MPA) is combined with Lambert W function to tackle the parameters extraction optimization problem for the single diode and double diode PV models and called (MPALW). The performance of the MPALW algorithm is tested by using real experimental data at seven sunlight and temperature settings. The MPALW shows an excellent agreement with obtained experimental data compared with other well-published algorithms. The findings of this research show that the MPALW algorithm can be utilized for real engineering applications such as smart grids, energy sector, and fault error detection.

1. Introduction

The efficient and accurate of the PV model is crucial for engineers and designers in order to refine the configuration of PV arrays with optimum solar energy usage (Khatib, 2015; H.M. Ridha et al., 2020b; Hussein Mohammed Ridha et al., 2020b). As consequence, improving the performance of the PV arrays leads to increase investments and creates more jobs. In the other side, the hazards of environmental pollutions and climate changes can be greatly reduced (Perera et al., 2020; Ridha et al., 2021). In general, the mathematical of the PV models can mainly be classified into three types: single diode, double diode, and three diode PV models (Khanna et al., 2015). The PV models' accuracy is strongly dependent on their parameters. It is therefore necessary to extract these parameters precisely with a high degree of efficiency (Abdulrazzaq et al., 2020; Nunes et al., 2019).

1.1. Literature review

The majority of PV models used in the literature are the single diode and dual diode models (Abbassi et al., 2018; Humada et al., 2020; Oliva et al., 2019). Various methods applied by the researchers for extraction

of the parameters of the PV models such as analytical, numerical, stochastic, and hybrid methods. The analytical methods present simple, fast, and accurate performance when the initial values are properly selected (Y. Chen et al., 2018; Gao et al., 2016). Additionally, these methods mainly use three key points: Open-circuit (OC), Short-circuit (SC), and Maximum Power Point (MPP) equations, which may sometimes be provided by manufacturers under standard test conditions (STC) (Batzelis and Papathanassiou, 2016; Chin et al., 2017; Chin and Salam, 2019a). Analytical methods can generally be categorized into approximate and exact methods (Dehghanzadeh et al., 2017; Lun et al., 2015). The approximate methods are straightforward and can be employed particularly to predict the output of the PV model using curve-fitting methods. While the exact explicit methods are assumed to be more efficient and could represent the actual performance especially in the high-voltage ranges (Çalasan et al., 2020; Y. Chen et al., 2018). The numerical methods are time-consuming and very susceptible to the initial values, which can easily fall in local minima such as Newton Raphson (NR) methods (Tossa et al., 2014), Levenberg Marquardt (LM) (Blaifi et al., 2019; Dkhichi et al., 2014), and piecewise I-V curve fitting method (Bai et al., 2014).

Recently, academics and researchers have utilized the stochastic methods in order to overcome the obstacles of the previous methods (X.

* Address at: Department of Electrical and Electronics Engineering, Faculty of Engineering, Universiti Putra Malaysia, 43400 Serdang, Malaysia.

E-mail addresses: hussain_mhammad@yahoo.com, gs46648@student.upm.edu.my.

Nomenclature	
d	ideality factor of diode
I_o	saturation current of the diode (A)
R_p	shunt resistance (Ω)
R_s	series resistance (Ω)
I_{ph}	photocurrent (A)
I_p	proposed current of the PV module (A)
V	voltage conducted by PV module (V)
I	current conducted by the PV module (A)
V_e	experimental voltage conducted by the PV module (V)
I_e	experimental current conducted by the PV module (A)
V_t	diode thermal voltage (V)
Tc	cell-temperature
$S_1 - S_7$	operational condition (solar radiation and cell temperature)
X_{min}	lower bounds of the population
X_{Max}	upper bound of the population
\vec{X}^k	vector of the top predator
Elite	Matrix for fittest solutions
Prey	matrix to update the position of predators
it	current iteration
Max_it	maximum iteration
R_B	Brownian motion is chosen within range [0,1]
R_L	represents Levy movement
v	velocity ratio
σ	Gaussian distribution
Γ	represents gamma function $\Gamma(1 + \alpha)$
KB	constant of Boltzmann (1.380603e-23 J/K)
AE	absolute error
RMSE	root mean square error
MBE	mean bias error
STD	standard deviation of RMSE
R^2	determination coefficient
STC	standard test condition
OC	Open-circuit
SC	Short-circuit
NR	Newton Raphson
LM	Levenberg Marquardt
TS	Taylor series
MPALW	Marine predator algorithm based on Lambert W function
SD, DD	Single diode and double diode PV model
PDE	penalty based differential evolution
IADE	improved adaptive DE.
SSA	salt swarm optimization
EO	Equilibrium optimizer
SMA	Slime mould algorithm
PSO	particle swarm optimization
DE	differential evolution
ABC	artificial bee colony
BHHO	boosted harris hawks optimizer
IEM	improved electromagnetism-like algorithm
DEAM	DE with adaptive mutation

Chen et al., 2019). These methods are known to be fast, accurate, excellent output in solving high-dimensional optimization problems, and do not restrict the initial values and objective function formulations (X. Chen et al., 2019). However, control parameters of these methods should be carefully calibrated for the possibility of stagnation to local minima. In comparison, each of these methods has weaknesses in the exploration and/or exploitation phases. A compromise between these two phases is therefore required to improve the efficiency of the PV system (Yang et al., 2020). Several stochastic methods were used in the literature such as Jaya Algorithm (Yu et al., 2019), Particle Swarm Optimization (PSO) (Liang et al., 2020), Differential Evolution (DE) (Yang et al., 2019), Coyote Optimization (CO) algorithm (Chin and Salam, 2019b), Electromagnetic-like (EM) Algorithm (H.M. Ridha et al., 2020a), Harries Hawks Optimization (HHO) (Abbassi et al., 2020; Hussein Mohammed Ridha et al., 2020c), Artificial Bee Colony (ABC) (Oliva et al., 2014), Ant Lion Optimizer (ALO) (Kanimozhi and Harish Kumar, 2018; Wu et al., 2017), Biogeography Based Optimization (BBO) method (Niu et al., 2014), Bacterial Fragging Algorithm (BFA) (Subudhi and Pradhan, 2018), Flower Pollination Algorithm (FPA) (Alam et al., 2015), Harmony Search (HS) (Askarzadeh and Rezazadeh, 2012), Firefly Algorithm (FA) (Louzazni et al., 2017), Fireworks Algorithm (FWA) (Sudhakar Babu et al., 2016), Multi-verso Optimizer (MVO) (Ali et al., 2016), Evaporation Rate Water Cycle Algorithm (EQ-WCA) (Kler et al., 2017), and Wind Driven Optimization (WDO) algorithm (Ibrahim et al., 2019), Brain Storming Optimization (BSO) algorithm (Yan et al., 2019), Bird Mating Optimizer (BMO) (Askarzadeh and Dos Santos Coelho, 2015), Salp Swarm Algorithm (Messaoud, 2020), Cat Swarm Optimization (CSO) (Guo et al., 2016) algorithm, Cuckoo Search (CS) (Kang et al., 2018), Moth Search Algorithm (MSA) (Fathy et al., 2019), Imperialist Competitive Algorithm (ICA) (Nassar-Eddine et al., 2016), Shuffled Complex Evolution (SCE) algorithm (Gao et al., 2018), Meta Rays Forging Optimizer (MRFO) (Selem et al., 2020), Generalized Oppositional Teaching Learning Based Optimization (GOTLBO) (Chen et al., 2016), Convolutional Neural Network (CNN) (Z. Chen et al.,

2019), and Transient Search Optimization (TSO) (Qais et al., 2020).

Dhiaa et al. proposed DE algorithm to solve the issue of the parameter extraction of the SD and DD PV models. DE with adaptive mutation (DEAM) algorithm was employed to determine 5-parameter of the PV module model and DE with integrated mutation per iteration (DEIM) algorithm was utilized to derive the DD PV module model's parameters. In the DEAM algorithm, the attraction–repulsion approach inspired by the EM algorithm was used to enhance the converge of the algorithm. In addition, new adjusting control parameters was proposed for each generation. Output findings have shown supremacy of DEAM method compared with penalty-based DE (PDE) algorithm proposed by (Ishaque et al., 2012) and improved adaptive DE (IADE) algorithm (Jiang et al., 2013), and Tamer's model (Khatib et al., 2013). Whilst, DEIM algorithm outperformed the proposed model by the authors of (Ishaque et al., 2011), Villalva et. al. (Villalva et al., 2009), Repaired adaptive DE (Rcr-IJADE) algorithm (Gong and Cai, 2013), IADE (Jiang et al., 2013), and PDE (Ishaque et al., 2012). However, DEAM and DEIM algorithms have several drawbacks such as the possibility of stagnation in local optimal especially when the optimization problem has multi-minima and also suffering from finding an optimal solution when the length used experimental data is large. In the other side, Hussein et. al proposed improved EM (IEM) (H.M. Ridha et al., 2020a) and boosted Harris Hawks Optimizer (BHHO) (Hussein Mohammed Ridha et al., 2020c) for extracting SD PV module's model parameters. In the IEM algorithm, two keys of improvements were introduced by employing nonlinear formula to adjust the particle's length in each iteration and total force calculation was simplified to enhance scanning new search regions. The IEM verified by using various statistical criteria using experimental data and compared with SSA, EM, Rcr-IJADE, IADE, PDE, and PSO algorithms. At the same time as BHHO technique has obtained spontaneous steps inspired by the Levy Flight (LF) concept for improving the diversity of the population. In addition, the mutation scheme of the DE algorithm integrated with the 2-opt technique was utilized to improve the potential of the convergence rate ability. BHHO has mastered several of the

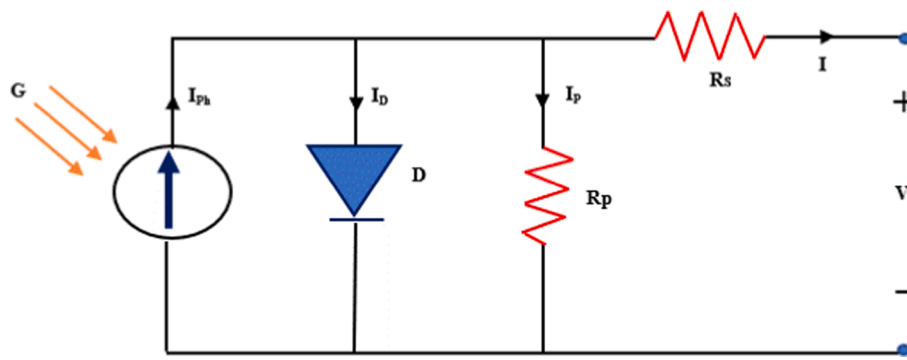


Fig. 1. The electrical circuit of the single-diode PV model.

methods mentioned in the literature.

In hybrid methods, by merging various algorithms or incorporating separate methodologies (numerical and analytical), hybrid algorithms can achieve reasonably high performance compared with the previous methods. Such techniques have been extensively employed for solving parameter optimization problems owing to their ability and high accuracy (Abbassi et al., 2019; X. Chen et al., 2018; Gnetchejo et al., 2019; Li et al., 2019; Qais et al., 2019; Rezaee Jordehi, 2018; Xu and Wang, 2017; Zhang et al., 2020). Nunes et al. (Nunes et al., 2018) proposed guaranteed convergence PSO (GCPSO) algorithm for determining the PV parameters of the SD and DD models using experimental data at various environmental conditions. A new velocity equation was scaled to monitor the search area around the global solution. According to the literature, the absence or limit of the real experimental data do not reflect the actual performance of the proposed methods in terms of reliability and accuracy. This is because the real experimental data have noises and high levels of variation in solar irradiance and temperature (Fébba et al., 2020). The most used experimental data: 67 mm dia RTC France SC under 1000 W/m² and 33 °C (Easwarakhanthan et al., 1986), Photo watt PWP-201 solar module under 1000 W/m² and 45 °C (Wu et al., 2018), Sharp ND-R250A5 solar module (Nunes et al., 2018), single-crystal 20 STM6-40/36 at 51 °C, and polycrystalline STM6-120/36 at 55 °C (Gao et al., 2018; Tong and Pora, 2016) are only under one weather condition. However, the experimental data of 67 mm dia RTC France SC (Easwarakhanthan et al., 1986) and Photo watt PWP-201 solar module under 1000 W/m² (Wu et al., 2018) were measured under 1000 W/m², which does not exist in real nature. It is worth to mention that the parameters optimization problem of the PV model can be formulated to minimize the error between proposed and experimental currents such as Root Mean Square Error (RMSE), Absolute Error (AR), and Mean bias Error (MBE). According to the literature, RMSE is the most indicator used as the main objective function to perform such task (Calasan et al., 2020).

1.2. Contribution

In this paper, a new meta-heuristic algorithms: Marine Predators Algorithm (MPA) combined with the Lambert W function (MPALW) is employed to solve parameters extraction optimization problem of the single diode and double diode models. Thus, the contributions of this paper can be summarized as follows:

- An effective MPALW method is developed to minimize the objective function.
- The new MPALW is used to extract the parameters of the SD and DD PV modules' models using real experimental data with regards to seven sunlight and temperature settings.
- MPALW is verified by using several statistical indicators and it is contrasted with other methods available in the literature.

2. Photovoltaic models and objective function

2.1. Single diode PV model

The single diode PV model's electrical equivalent circuit is illustrated in Fig. 1. In general, there are five physical parameters comprised SD PV model: a current source I_{ph} in (A) connected in parallel, diode ideality factor d connected oppositely to represent the output voltage of the PV cells, the saturation current of the diode I_o in (A), large shunt resistance R_p in (Ω) connected in parallel to describe the diode's saturation current, and small series resistance R_s in (Ω). The output current I in (A) of the PV cell can be computed by using Kirchhoff's law and given by,

$$I = I_{ph} - I_d - I_p, \quad (1)$$

where I_d is the forward diode current in (A) and I_p is the shunt resistor current in (A). Thus, I_d can be calculated by utilizing the Shockley diode law as follows:

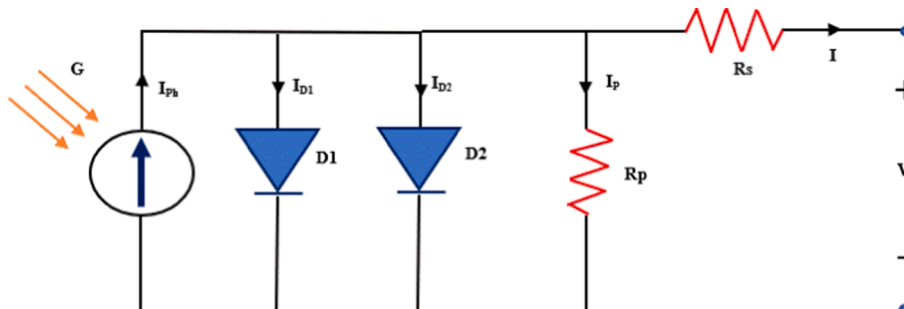


Fig. 2. The electrical circuit of the double-diode PV model.

$$I_d = I_o \left[\exp\left(\frac{V + IR_s}{V_t}\right) - 1 \right], \quad (2)$$

where V refers to the output voltage (V) and V_t is the diode's thermal voltage (V) and can be written by the following:

$$V_t = \frac{dKBT_c}{q}, \quad (3)$$

where KB represents the constant of Boltzmann ($1.38 \times 10^{-23} J/K$), T_c is the cell temperature (K), and q is the electron charge ($1.60 \times 10^{-19} C$). The I_p can be given as follows:

$$I_p = \frac{V + IR_s}{R_p}, \quad (4)$$

by solving Eqs. (1)-(4), the I is represented by the following equation:

$$I = I_{ph} - I_o \left[\exp\left(\frac{V + IR_s}{V_t}\right) - 1 \right] - \frac{V + IR_s}{R_p}, \quad (5)$$

Note that the five parameters are subject to operating conditions (solar irradiance and cell temperature). However, the PV arrays that consist of N_s modules are coupled in series to upturn the output voltage, and N_p modules are connected in parallel to increase the output current. Therefore, the output current of the PV arrays can be computed as (Muhsen et al., 2015a):

$$I = N_p I_{ph} - N_p I_o \left[\exp\left(\frac{1}{V_t} \left(\frac{V}{N_s} + \frac{IR_s}{N_p} \right)\right) - 1 \right] - \frac{N_p}{R_p} \left(\frac{V}{N_s} + \frac{IR_s}{N_p} \right), \quad (6)$$

2.2. Double-diode PV model

The double diode PV model's electrical equivalent circuit is depicted in Fig. 2. The key benefit of using the DD PV model is offered better accuracy when the solar irradiance levels are low. The d_2 is added to describe the recombination losses, which occur in the depletion region. Thus, the DD PV model's output current is given by (Muhsen et al., 2015b):

$$I = I_{ph} - I_{o1} \left[\exp\left(\frac{V + IR_s}{V_{t1}}\right) - 1 \right] - I_{o2} \left[\exp\left(\frac{V + IR_s}{V_{t2}}\right) - 1 \right] - \frac{V + IR_s}{R_p}, \quad (7)$$

where I_{o1} and I_{o2} are the diode reverse saturation currents (A), and V_{t1} and V_{t2} are the diode thermal voltages (V) expressed by:

$$V_{t1} = \frac{d_1 KBT_c}{q}, \quad (8)$$

$$V_{t2} = \frac{d_2 KBT_c}{q}, \quad (9)$$

where d_1 and d_2 are the first and second diodes' ideality factors. Although the DD PV module has high accuracy, it needs extensive computation to determine the seven parameters of the DD model (I_{ph} , I_{o1} , I_{o2} , R_s , R_p , d_1 and d_2).

2.3. Objective function

The aim of model construction and parameter extraction is to minimize the error between the computed and experimental currents at various environmental conditions. As a consequence, the estimation of the five and seven parameters can be formulated by using RMSE as an objective function that needs to be minimized.

In the literature, solving the nonlinear equation of the PV model can be performed either by using numerical computations or by utilizing linear equation. Therefore, applying a reliable and accurate methodology is

very important to extract the parameters of the PV models (Yousri et al., 2020). It is relevant to note that Eqs. (7 and 6) are nonlinearity implicit transcendental equations and have five and seven unknown parameters. In fact, there are several studies proposed methods to optimally extract these parameters such as LM (Tossa et al., 2014), NR (Abbassi et al., 2017; Muhsen et al., 2015b), Taylor series (TS) (Lun et al., 2013), and Lambert W function (Tossa et al., 2014). In this study, two methods are carried out for estimating the parameters of the PV models, which are the Newton Raphson method and the Lambert W function method as follows:

2.3.1. Newton Raphson method

To estimate the five parameters and seven parameters of the PV models at specific weather conditions, the NR method is used for solving I-V curve equations which can be given by the following (Muhsen et al., 2015b, 2015a; Nassar-Eddine et al., 2016; H.M. Ridha et al., 2020a; Hussein Mohammed Ridha et al., 2020c):

For the SD PV model:

$$I = I - \left(\frac{I_{ph} - I - I_o \left(\exp\left(\frac{V+R_s I}{dV_t}\right) - 1 \right) - \frac{V+R_s I}{R_p}}{-1 - I_o \left(\frac{R_s}{dV_t} \right) \exp\left(\frac{V+R_s I}{dV_t}\right) - \frac{R_s}{R_p}} \right), \quad (10)$$

For the DD PV model:

$$I = I - \left(\frac{I_{ph} - I - I_{o1} \left(\exp\left(\frac{V+R_s I}{d_1 V_t}\right) - 1 \right) - I_{o2} \left(\exp\left(\frac{V+R_s I}{d_2 V_t}\right) - 1 \right) - \frac{V+R_s I}{R_p}}{-1 - I_{o1} \left(\frac{R_s}{d_1 V_t} \right) \exp\left(\frac{V+R_s I}{d_1 V_t}\right) - I_{o2} \left(\frac{R_s}{d_2 V_t} \right) \exp\left(\frac{V+R_s I}{d_2 V_t}\right) - \frac{R_s}{R_p}} \right), \quad (11)$$

2.3.2. Lambert W function method

To mitigate the implicit coupling relation between the voltage and current, the Lambert W function is employed for this role. Therefore, the Lambert W function is used to optimally extract the parameters of the SD and DD PV models owing to the high accuracy, among other methods, and the usage of heterogeneous operating temperatures (Calasan et al., 2020; Y. Chen et al., 2018; Fébba et al., 2020; Ghani et al., 2014). Therefore, the output current of the SD and DD modules based on Lambert W function can be expressed as:

For the SD PV model:

$$I = \frac{R_p(I_{ph} + I_o) - V}{R_p + R_s} - \frac{V_t}{R_s} [dW(\beta)], \quad (12)$$

where

$$\beta = \frac{I_o R_s R_p}{dV_t (R_s + R_p)} \exp\left\{ \frac{R_p(R_s I_{ph} + R_s I_o + V)}{dV_t (R_s + R_p)} \right\}, \quad (13)$$

For the DD PV model:

$$I = \frac{R_p(I_{ph} + I_{o1} + I_{o2}) - V}{R_p + R_s} - \frac{V_t}{R_s} [d_1 W(\beta_1) + d_2 W(\beta_2)], \quad (14)$$

where

$$\beta_1 = \frac{I_{o1} R_s R_p}{d_1 V_{t1} (R_s + R_p)} \exp\left\{ \frac{R_p(R_s I_{ph} + R_s I_{o1} + V)}{d_1 V_{t1} (R_s + R_p)} \right\}, \quad (15)$$

$$\beta_2 = \frac{I_{o2} R_s R_p}{d_2 V_{t2} (R_s + R_p)} \exp\left\{ \frac{R_p(R_s I_{ph} + R_s I_{o2} + V)}{d_2 V_{t2} (R_s + R_p)} \right\}, \quad (16)$$

Thus, the objective function can be written as follows:

$$RMSE = \sqrt{\frac{1}{N} \sum_{i=1}^N P(V_e, I_e, \theta)^2}, \quad (17)$$

where N is the length of the I-V data curve, V_e and I_e are the experimental voltage and current of the PV model, while θ refers to the vector of the parameters that required to be optimally extracted.

3. Marine Predators Algorithm

MPA is a novel nature-inspired meta-heuristic algorithm proposed by Afshin et al. in 2020 (Faramarzi et al., 2020). MPA is inspired by the widespread foraging strategy of the Levy and Brownian motions in ocean predators combining with encounter rate policy by following marine ecosystems between the prey and predator. Like other meta-heuristic algorithms, MPA uniformly distributed initial solution over search space.:

3.1. Initialization

$$X_i = X_{Min} + rnd(X_{Max} - X_{min}), \quad (18)$$

where rnd is a random value within range [0,1], and $(X_{Max}$ and X_{min}) are upper and lower variables of a population.

According to the *survival of the fittest theory*, the fittest solution is chosen as a top predator, which is used to establish a matrix named to Elite. These arrays are responsible for finding and searching the preys based on prior information on their positions.

$$Elite = \begin{bmatrix} X_{1,1}^K X_{1,2}^K \cdots X_{1,z}^K \\ X_{2,1}^K X_{2,2}^K \cdots X_{2,z}^K \\ \vdots \vdots \vdots \\ X_{m,1}^K X_{m,2}^K \cdots X_{m,z}^K \end{bmatrix}_{m,z}, \quad (19)$$

where $\overrightarrow{X^K}$ is the vector of the top predator, and it is replicated m times in order to construct the *Elite* matrix. The parameter m represents the search agents' number, and z denotes the number of dimensions. In this algorithm, the predator and prey are used as search agents in which each one is looking for its prey or own food. Consequently, the *Elite* is updated if there is a new fittest predator. In meanwhile, the *Prey* matrix is used to update the positions of the predators and can be given by follows:

$$Prey = \begin{bmatrix} X_{1,1} X_{1,2} \cdots X_{1,z} \\ X_{2,1} X_{2,2} \cdots X_{2,z} \\ \vdots \vdots \vdots \\ X_{m,1} X_{m,2} \cdots X_{m,z} \end{bmatrix}_{m,z}, \quad (20)$$

where X_{ij} is the j -th dimension of the i -th prey. It is worth to mention that the whole process of the optimization is mainly depended on the *Elite* and *Prey* matrices.

3.2. MPA optimization procedures

The MPA optimization process consists mainly of three phases, taking into account various velocity ratios, mimicking the nature life of a predator and prey at the same time:

- When the motion of the prey is faster than the predator (in the high-velocity ratio).

- When the motion of the prey and predator are at the same pace (in the unit velocity).
- When the motion of the predator is faster than the prey (in the low velocity).

In each phase, there is a specific number of iterations in order to simulate the entire life of predator and prey in nature. The three steps are:

When the moving of the prey is faster than the predator or in the high-velocity ratio ($v \geq 10$). This phase presents the initialization of the optimization process specifically for exploration matters. This phase occurs in the first third of the iterations. The equation that describes this phase can be applied as follows:

$$\begin{aligned} & \text{while } it < \frac{1}{3} Max_it \\ & \overrightarrow{\text{stepsize}}_t = \overrightarrow{R_B} \otimes (\overrightarrow{\text{Elite}}_t - \overrightarrow{R_B} \otimes \overrightarrow{\text{Prey}}_t) \quad t = 1, \dots, m \\ & \overrightarrow{\text{Prey}}_t = \overrightarrow{\text{Prey}}_t + P \cdot \overrightarrow{R} \otimes \overrightarrow{\text{stepsize}}_t \end{aligned} \quad (21)$$

where it is the current iteration and Max_it is the maximum one. R_B is randomly numbers vector chosen based on the Normal distribution to represent the Brownian motion. The symbol \otimes refers to the entry-wise multiplications. Thus, the multiplication of $\overrightarrow{\text{Prey}}_t$ by the $\overrightarrow{R_B}$ shows the motion of the prey. \overrightarrow{R} is randomly chosen number within range [0,1], and P is set to be constant at 0.5.

When the motion of the prey and predator are at the same pace or in unit velocity ($v \approx 1$). In this phase, the optimization process is shifted from exploration to exploitation which half of the population (prey) is divided for exploration, and the second half (predators) is designed for exploitation. According to the rule, if the movement of the prey in Levy, the best motion for a predator is Brownian. The first half is given by the following:

$$\begin{aligned} & \text{while } \frac{1}{3} Max_it < it < \frac{2}{3} Max_it \\ & \overrightarrow{\text{stepsize}}_t = \overrightarrow{R_L} \otimes (\overrightarrow{\text{Elite}}_t - \overrightarrow{R_L} \otimes \overrightarrow{\text{Prey}}_t) \quad t = 1, \dots, m/2 \\ & \overrightarrow{\text{Prey}}_t = \overrightarrow{\text{Prey}}_t + P \cdot \overrightarrow{R} \otimes \overrightarrow{\text{stepsize}}_t, \end{aligned} \quad (22)$$

where $\overrightarrow{R_L}$ is a vector randomly selected based on Levy's strategy to mimic the Levy movement. Multiplication of $\overrightarrow{R_B}$ by $\overrightarrow{\text{Prey}}_t$ shows the motion of the prey in levy step size. Whist, the second half of this phase, concludes:

$$\begin{aligned} & \overrightarrow{\text{stepsize}}_t = \overrightarrow{R_B} \otimes (\overrightarrow{R_B} \otimes \overrightarrow{\text{Elite}}_t - \overrightarrow{\text{Prey}}_t) \quad t = m/2, \dots, m \\ & \overrightarrow{\text{Prey}}_t = \overrightarrow{\text{Elite}}_t + P \cdot CF \otimes \overrightarrow{\text{stepsize}}_t, \end{aligned} \quad (23)$$

where $CF = \left(1 - \frac{it}{Max_it}\right)^{\left(\frac{2}{Max_it}\right)}$ is an adaptive parameter for controlling the step size of the predator motion. Multiplication of $\overrightarrow{R_B}$ by $\overrightarrow{\text{Elite}}_t$ to

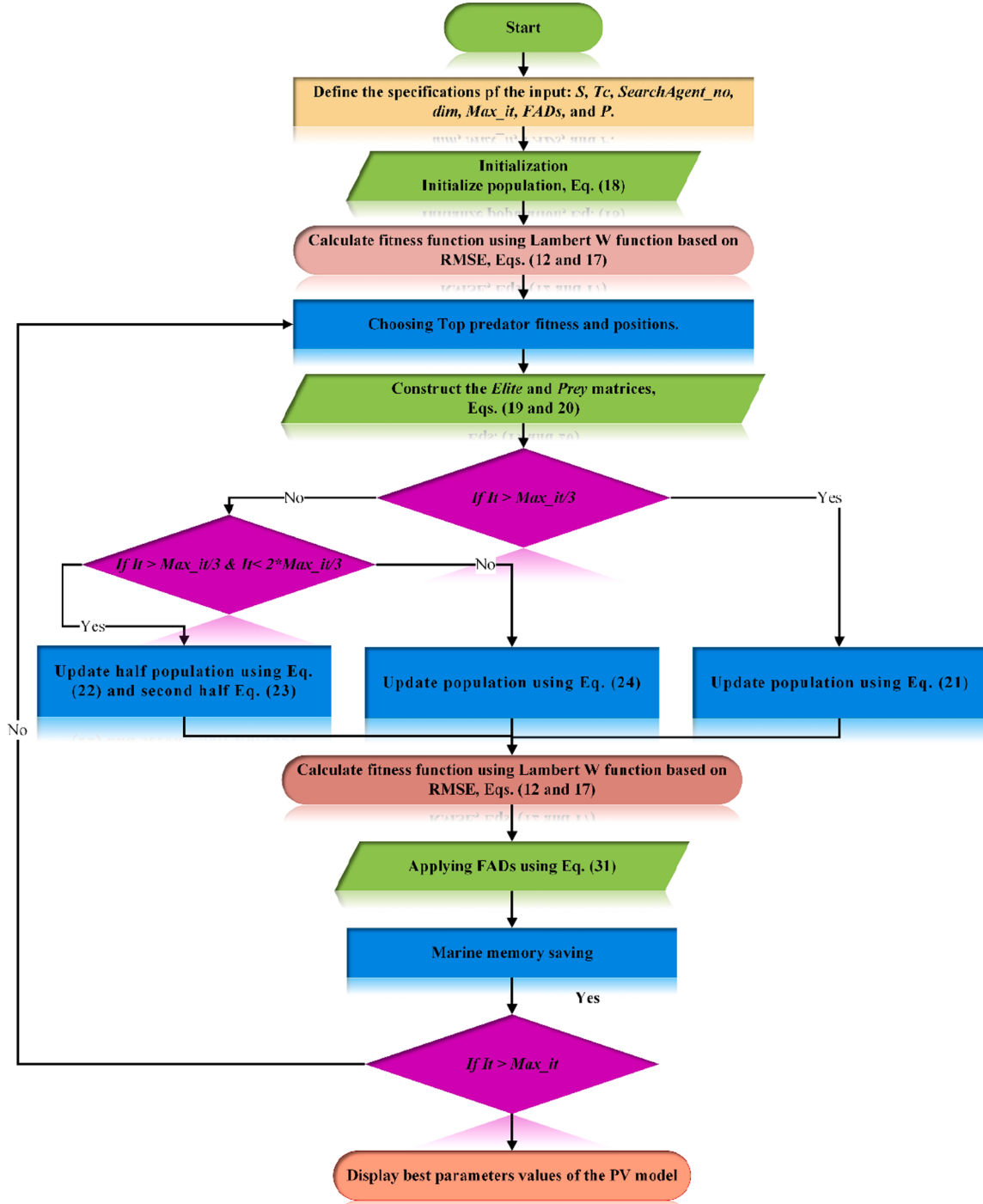
**Fig. 3.** Flowchart of the proposed MPALW algorithm.

Table 1

Multi-crystalline Kyocera (KC120-1) PV module specification.

Characteristics	Value
Maximum power at STC (P_{max}) in (W_p)	120
Open-circuit voltage (V_{oc}) in (V)	21.5
Short-circuit current (I_{sc}) in (A)	7.45
Voltage at MPP (V_{mp}) in (V)	16.9
Current at MPP (I_{mp}) in (A)	7.1
Nominal Operation Cell Temperature (NOCT) in (°C)	43.6
Number of cells connected in series	36
Temperature coefficient of I_{sc} (α) in (mA/k)	1.325
Temperature coefficient of V_{sc} (β) in (mV/k)	-77.5

demonstrates the motion of the predators in Brownian step size.

When the motion of the predator is faster than prey or in low velocity ($v = 0.1$). This phase occurs at the last stage of the optimization process when an extensive exploitation capability is required. This phase can be presented as follows:

$$\text{while } it < \frac{2}{3} \text{Max_it}$$

$$\overrightarrow{\text{stepsize}_t} = \overrightarrow{R_L} \otimes \left(\overrightarrow{R_L} \otimes \overrightarrow{\text{Elite}_t} - \overrightarrow{\text{Prey}_t} \right) t = 1, \dots, m$$

$$\overrightarrow{\text{Prey}_t} = \overrightarrow{\text{Elite}_t} + P.CF \otimes \overrightarrow{\text{stepsize}_t}, \quad (24)$$

The predator's movement in Levy strategy is simulated by multiplications of $\overrightarrow{R_L}$ by $\overrightarrow{\text{Elite}_t}$ while the step size is added to $\overrightarrow{\text{Elite}_t}$ position to simulate the predator's movement to assist the update of prey position. The description of the two randomly walks of Brownian and Levy movements are given by,

Brownian motion: It is a stochastic step size process inspired by Gaussian distribution with unit variance ($\sigma^2 = 1$) and zero mean ($\mu = 0$). For this motion, the Probably Density Function (PDF) at point x is given by following (Einstein, 1956):

$$f_B(x, \mu, \sigma) = \frac{1}{\sqrt{2\pi\sigma^2}} \exp\left(-\frac{(x-\mu)^2}{2\sigma^2}\right) = \frac{1}{\sqrt{2\pi}} \exp\left(\frac{x^2}{2}\right), \quad (25)$$

Levy flight: is the second type of randomly step sizes are chosen based on a probability function determined by Levy distribution:

$$L(x_j) \approx |x_j|^{1-\alpha} \quad (26)$$

where x_j is the length of the flight, and the exponent of the power-law is $1 < \alpha < 2$ (Humphries et al., 2010). The probability density of the Levy distribution in integral form can be written as (Mantegna, 1994):

$$f_L(x, \mu, \sigma) = \frac{1}{\pi} \int_0^\infty \exp(-\gamma q^\alpha) \cos(qx) dq \quad (27)$$

where α is the distribution index that can control the scale properties of the process. γ is used to select the scale unit. The integral is used when the $\alpha = 2$ representing Gaussian distribution and when $\alpha = 1$ representing a Cauchy distribution (Yang, 2010). A series expansion method is required when x has a huge value as shown by the following:

Table 3

The search range of the SD and DD PV models.

Parameter	Single/double diode	
	LB	UB
d_1, d_2	1	2
I_{ph}	0.5	8
I_{o1}, I_{o2}	$1e^{-12}$	$1e^{-5}$
R_s	0.1	2
R_p	10	8000

$$f_L(x, \mu, \sigma) = \frac{\gamma \Gamma(1+\alpha) \sin\left(\frac{\pi\alpha}{2}\right)}{\pi x^{1+\alpha}}, \quad x = \infty \quad (28)$$

where Γ represents gamma function in which $\Gamma(1+\alpha)$ is equal to $\alpha!$. According to (Mantegna, 1994), the value of α ranged within 0.3 and 1.99. In this study, the Mantegna method is used to generate a random number using Levy distribution as shown by the following:

$$\text{Levy}(\alpha) = 0.05 \times \frac{x}{|y|^{1/\alpha}} \quad (29)$$

where y and x two normal distribution variables which can be written as follows:

$x = \text{Normal}(0, \sigma_x^2)$, and $y = \text{Normal}(0, \sigma_y^2)$, where the σ_x is computed as follows:

$$\sigma_x = \left[\frac{\Gamma(1+\alpha)n\left(\frac{\pi\alpha}{2}\right)}{\Gamma\left(\frac{(1+\alpha)}{2}\right)\alpha 2^{\left(\frac{\alpha-1}{2}\right)}} \right]^{1/\alpha}, \text{ where, } \sigma_y = 1 \text{ and } \alpha = 1.5. \quad (30)$$

The Levy strategy has movements with small steps size combined with long jumps, while the Brownian has the ability to cover most of the regions within the domain associated with uniform and controlled step size (Yang, 2010).

3.3. Eddy formation and effect of FAD

Another point of view to mimic the natural behavioural change in marine predators, such as the eddy formation and effects of the Fish Aggregation Devices (FADs). The authors of (Fil malter et al., 2011) studied that 80% of their time spend by sharks near FADs and 20% will be spent for the long jump in various search spaces which lead to local minima avoidance as presented by,

$$\overrightarrow{\text{Prey}_t} \begin{cases} \overrightarrow{\text{Prey}_t} + CF[\overrightarrow{X_{min}} + \overrightarrow{R} \otimes (\overrightarrow{X_{max}} - \overrightarrow{X_{min}}) \otimes \overrightarrow{U}] if s \leq FADs \\ \overrightarrow{\text{Prey}_t} + [FADs(1-s) + s](\overrightarrow{\text{Prey}_{s1}} - \overrightarrow{\text{Prey}_{s2}}) if s > FADs \end{cases} \quad (31)$$

where $\overrightarrow{X_{max}}$ and $\overrightarrow{X_{min}}$ are vectors of upper and lower bounds dimensions, \overrightarrow{U} is a binary number with arrays ranged 0 and 1 which it can change the array to zero if the array < 0.2 and to 1 if the array > 0.2 , $FADs$ represents the probability of FADs effect, $S1$ and $S2$ are random indexes of Prey matrix, and S is a random number within range [0,1].

Table 2

Data points of experimental (I-V) curve for different operational conditions (Muhsen et al., 2015b).

Environmental condition	S_1	S_2	S_3	S_4	S_5	S_6	S_7
Length of data points (N)	22	24	50	91	92	101	102
Solar irradiance (W/m^2)	118.28	148	306	711	780	840	978
Cell temperature (K)	318.32	321.25	327.7	324.21	329.1	331.42	328.56

Table 4

Extracted parameters of the MPALW algorithm and other algorithms for the SD PV model.

Parameters	Method	S_1	S_2	S_3	S_4	S_5	S_6	S_7
d	MPALW	1.2700	1.3898	1.1891	1.3178	1.2967	1.3495	1.3771
	MPA	1.1130	1.4251	1.2073	1.3167	1.3257	1.3495	1.3750
	IEM	1.1283	1.4443	1.1766	1.2542	1.3059	1.3305	1.3257
	BHHO	1.1235	1.2142	1.0306	1.3000	1.1951	1.3489	1.3542
	DEAM	1.1010	1.4290	1.1680	1.2775	1.3140	1.3495	1.3771
	EO	1.4205	1.4989	1.2512	1.2431	1.3446	1.3492	1.3772
	SMA	1.0019	1.4716	1.0000	1.3519	1.3798	1.3224	1.2854
I_{ph}	MPALW	0.8382	0.9352	1.9472	4.4173	5.1539	5.1856	6.4692
	MPA	0.8397	0.9257	1.9334	4.4237	5.1497	5.1849	6.4777
	IEM	0.8419	0.9063	1.9483	4.4128	5.1145	5.1485	6.3930
	BHHO	0.8427	1.0228	1.9321	4.4170	5.0840	5.1522	6.3396
	DEAM	0.8393	0.9220	1.9545	4.4242	5.1469	5.1859	6.4691
	EO	0.8507	0.9149	1.9374	4.4176	5.1121	5.1537	6.4380
	SMA	0.8801	0.9055	1.9130	4.4281	4.9470	5.1543	6.4124
I_o	MPALW	1.43E-07	3.98E-06	9.89E-07	3.75E-06	4.17E-06	1.00E-05	1.00E-05
	MPA	1.17E-07	5.44E-06	1.23E-06	3.71E-06	5.67E-06	1.00E-05	9.80E-06
	IEM	1.45E-07	6.46E-06	8.43E-07	1.82E-07	4.60E-06	8.29E-06	5.91E-06
	BHHO	1.36E-07	6.29E-07	1.03E-07	3.09E-06	1.26E-06	9.96E-06	8.13E-06
	DEAM	9.76E-08	5.65E-06	7.57E-07	2.39E-06	5.01E-06	1.00E-05	1.00E-05
	EO	3.69E-06	9.97E-06	2.05E-06	1.59E-06	6.92E-06	9.99E-06	9.99E-06
	SMA	1.95E-08	8.09E-06	6.25E-08	5.38E-06	9.99E-06	7.57E-06	3.83E-06
R_s	MPALW	1.7270	0.2729	0.6665	0.5173	0.2756	0.1975	0.1863
	MPA	1.7829	0.2352	0.6653	0.5149	0.2678	0.1977	0.1847
	IEM	1.7880	0.2370	0.6656	0.5416	0.2801	0.2062	0.2140
	BHHO	1.7279	0.3937	0.7914	0.5240	0.3196	0.2006	0.1851
	DEAM	1.7772	0.2495	0.6623	0.5278	0.2707	0.1975	0.1863
	EO	1.2078	0.1435	0.6317	0.5506	0.2676	0.2008	0.1941
	SMA	1.7973	0.1546	0.8221	0.5091	0.2862	0.2151	0.2187
R_p	MPALW	7989.79	342.63	508.44	239.93	41.68	312.72	30.29
	MPA	7999.99	514.73	4495.31	200.64	43.51	319.44	29.36
	IEM	7568.35	7833.33	367.96	199.95	50.12	7935.04	38.51
	BHHO	1873.90	88.34	383.49	223.43	54.05	5748.70	40.65
	DEAM	1151.77	751.37	284.28	167.91	43.29	309.12	30.30
	EO	6551.01	1505.62	4979.27	201.07	52.99	7951.47	34.22
	SMA	204.08	6171.26	1257.31	280.42	3652.26	3516.22	34.29

3.4. Marine memory

MPA uses memory to update the Elite, where each solution of the current iteration is compared with the prior one, and the fittest solution is chosen for the next iteration. The flowchart of the MPALW algorithm is shown in Fig. 3.

4. Results and discussions

In this research paper, the Marine Predator Algorithm is combined with Lambert W function (MPALW) to identify the unknown parameters of SD and DD using experimental data of Kyocera KC120-1 multi-crystalline PV module model. The PV specifications at STC are given in Table 1. While the numbers of I-V data points under various environmental conditions are Tabulated in Table 2 (Muhsen et al., 2015b). The proposed MPA-LW is verified by using experimental data under seven weather condition (S_1 – S_7) and several statistical criteria. Moreover, MPALW algorithm compared with MPA proposed by Faramarzi et. al. (Faramarzi et al., 2020), IEM (H.M. Ridha et al., 2020a), BHHO (Hussein Mohammed Ridha et al., 2020c), DEAM (Muhsen et al., 2015a), EO (Faramarzi et al., 2019), and Slime mould algorithm (SMA) (Li et al., 2020) algorithms for the SD PV model. While the same algorithms are compared MPALW algorithm for the DD PV model except the DEIM algorithm is used (Muhsen et al., 2015b) instead of the DEAM algorithm. These algorithms are chosen due to the same experimental data were obtained to solve this optimization problem.

For fair comparisons, the dimension of the optimization problem of the SD and DD PV models are five and seven, respectively. The population size is set to be 30, and the maximum iteration number is set to be 250. The search space of the SD and DD PV models' parameters are tabulated in Table 3 (Muhsen et al., 2015b; Hussein Mohammed Ridha

et al., 2020c).

4.1. Results on single diode PV module

The results of the extracted parameters for the SD PV module model based on MPALW and other algorithms under various sunlight and temperature conditions are demonstrated in Table 4. Fig. 4 (a and b) exhibits the I-V and P-V characteristics curves between measured and computed data of the SD PV module model for the MPALW and other algorithms. The PV crystalline PV module has a sharp I-V curve due to the large value of the R_p and a smaller value of the PV module has a sharp I-V curve due to the large value of the R_s . According to these figures, the proposed MPALW method and other methods are closed to the real experimental data, except for SMA and BHHO, especially at high levels of irradiance and temperature. Thus, it can be confirmed that the performance of these models is influenced by the variation of the weather conditions and the existence of the noise associated with experimental data.

A detailed comparison of the proposed MPALW with MPA, IEM, BHHO, DEAM, EO, and SMA algorithms for the SD PV module model is given in Table 5. The performance results of Table 5 indicate the superiority of the MPALW, among other algorithms followed by DEAM and MPA, respectively. The average RMSE of these models is 0.0581, 0.0582, and 0.0582, respectively. It is worth noting that MPA and DEAM have the same accuracy based on the NR method. However, MPALW demonstrated that Lambert W function has more ability to determine the parameters of the SD PV model. While the worst RMSE values were found by BHHO, and SMA, particularly at a high level of solar irradiance and ambient temperature. The similar performance can be observed using statistical criteria: MBE and R^2 , where average values of the MPALW are 0.0049 and 0.9944, respectively. It is clear that SMA has less

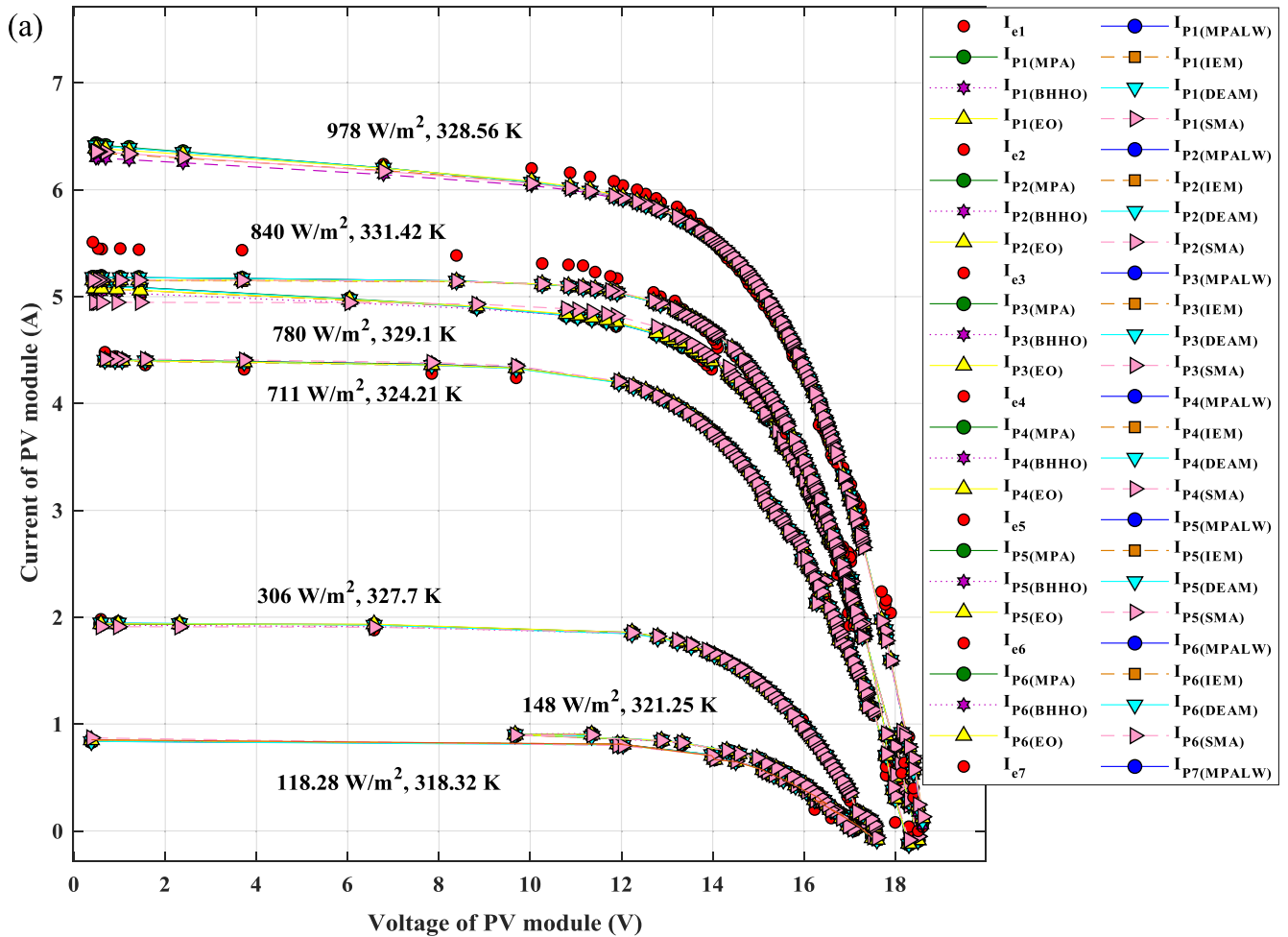


Fig. 4. Comparison between the computed and experimental data of the MPALW and other models. (a) I-V curve and (b) P-V curve.

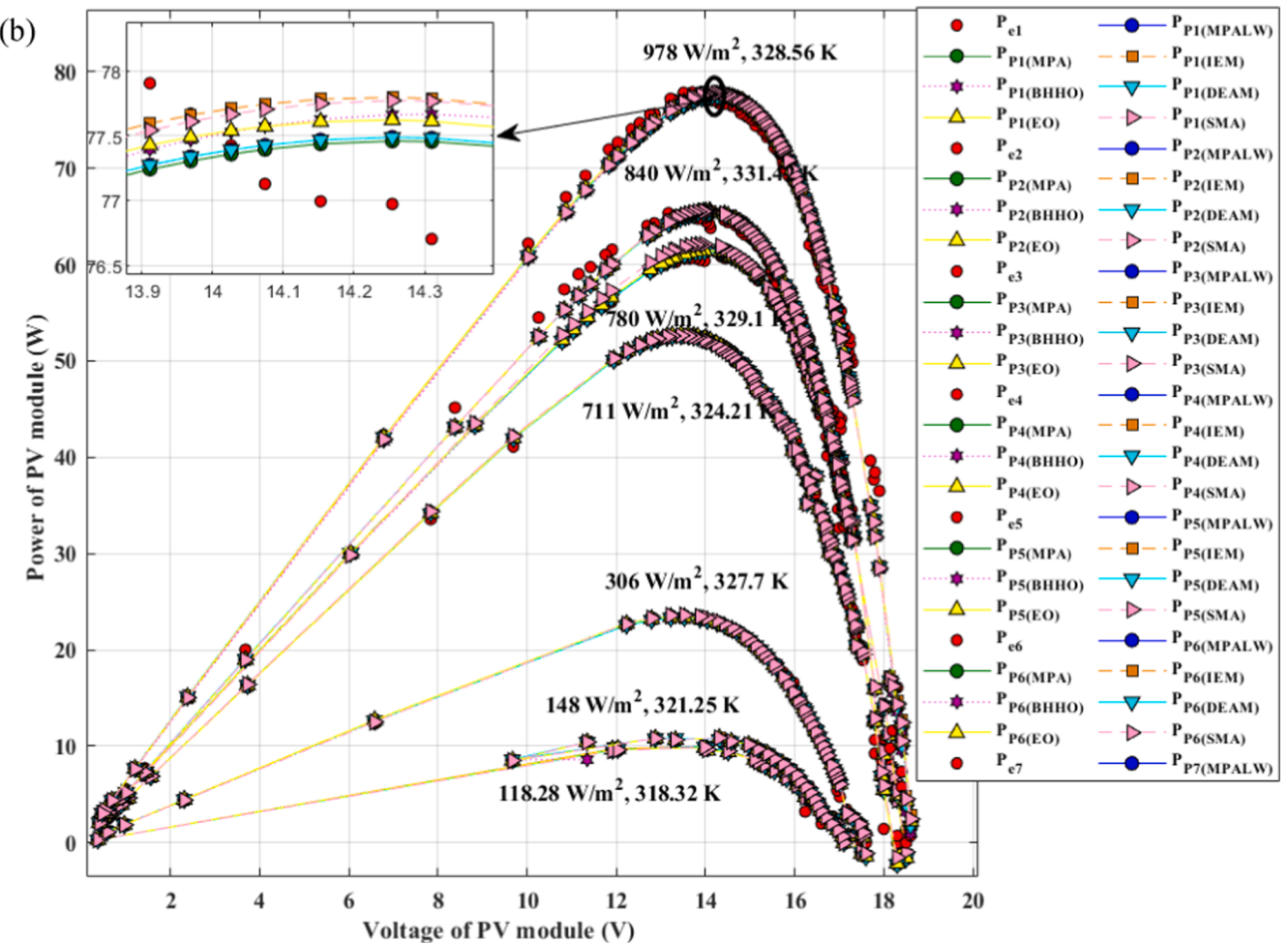


Fig. 4. (continued).

Table 5

RMSE, MBE, and R^2 of the proposed MPALW and other algorithms for the SD PV model.

Parameters	Method	S_1	S_2	S_3	S_4	S_5	S_6	S_7	Average
RMSE	MPALW	0.0333	0.0132	0.0270	0.0287	0.0908	0.0882	0.1255	0.0581
	MPA	0.0332	0.0133	0.0276	0.0287	0.0909	0.0882	0.1257	0.0582
	IEM	0.0333	0.0134	0.0268	0.0284	0.0913	0.0891	0.1299	0.0589
	BHHO	0.0333	0.0128	0.0267	0.0286	0.0934	0.0885	0.1306	0.0591
	DEAM	0.0342	0.0136	0.0267	0.0284	0.0908	0.0882	1.2559	0.0582
	EO	0.0346	0.0134	0.0278	0.0285	0.0914	0.0885	0.1259	0.0586
	SMA	0.0339	0.0135	0.0283	0.0295	0.1040	0.0895	0.1313	0.0614
MBE	MPALW	0.0011	0.0001	0.0007	0.0008	0.0082	0.0077	0.0157	0.0049
	MPA	0.0011	0.0001	0.0007	0.0008	0.0082	0.0077	0.0158	0.0049
	IEM	0.0001	0.0001	0.0007	0.0008	0.0083	0.0079	0.0168	0.0051
	BHHO	0.0011	0.0001	0.0007	0.0008	0.0087	0.0078	0.0170	0.0052
	DEAM	0.0011	0.0001	0.0007	0.0008	0.0082	0.0077	0.0150	0.0049
	EO	0.0001	0.0001	0.0007	0.0008	0.0083	0.0078	0.0158	0.0050
	SMA	0.0011	0.0001	0.0008	0.0087	0.0108	0.0080	0.0172	0.0055
R^2	MPALW	0.9832	0.9977	0.9978	0.9993	0.9949	0.9955	0.9932	0.9944
	MPA	0.9832	0.9977	0.9977	0.9993	0.9949	0.9955	0.9932	0.9944
	IEM	0.9831	0.9976	0.9978	0.9993	0.9948	0.9955	0.9927	0.9944
	BHHO	0.9832	0.9978	0.9979	0.9993	0.9946	0.9955	0.9926	0.9944
	DEAM	0.9822	0.9975	0.9979	0.9993	0.9949	0.9955	0.9932	0.9944
	EO	0.9817	0.9976	0.9977	0.9993	0.9948	0.9955	0.9932	0.9932
	SMA	0.9825	0.9976	0.9976	0.9992	0.9933	0.9954	0.9926	0.9940

accuracy and stability than other methods.

According to Fig. 5, the visualization of the RMSE values at arbitrary weather conditions shows the worst RMSE value at each level cues by intensity color, while the best value of RMSE is indicated by hue color. By starting with dark blue color, the methods almost have trivial

differences at S_1 , S_2 , S_3 , and S_4 . This is due to the few data points of the real experimental data. However, the distinct color can obviously be seen by the BHHO and SMA methods compared with other methods at S_5 . Similar manner can be shown at S_6 using IEM and SMA methods. At S_7 , the MPALW, MPA, DEAM, and EO methods have approximately

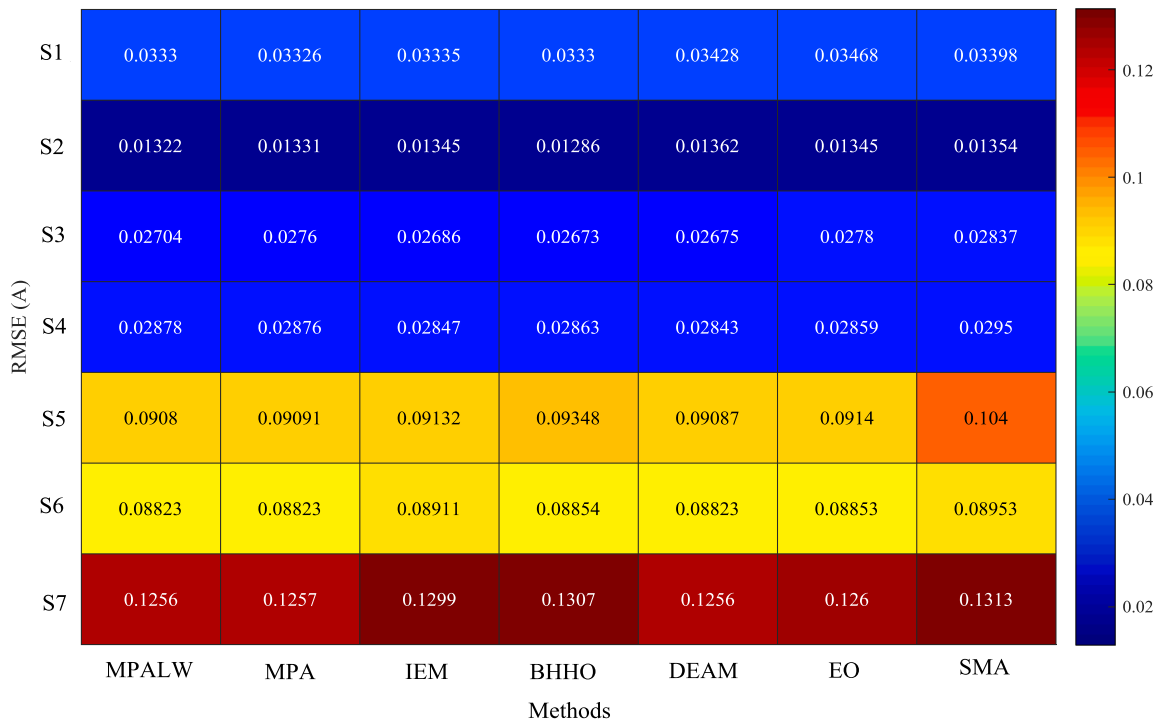


Fig. 5. Heatmap demonstrates the variation of the RMSE values with solar radiations among several methods for the SD PV model.

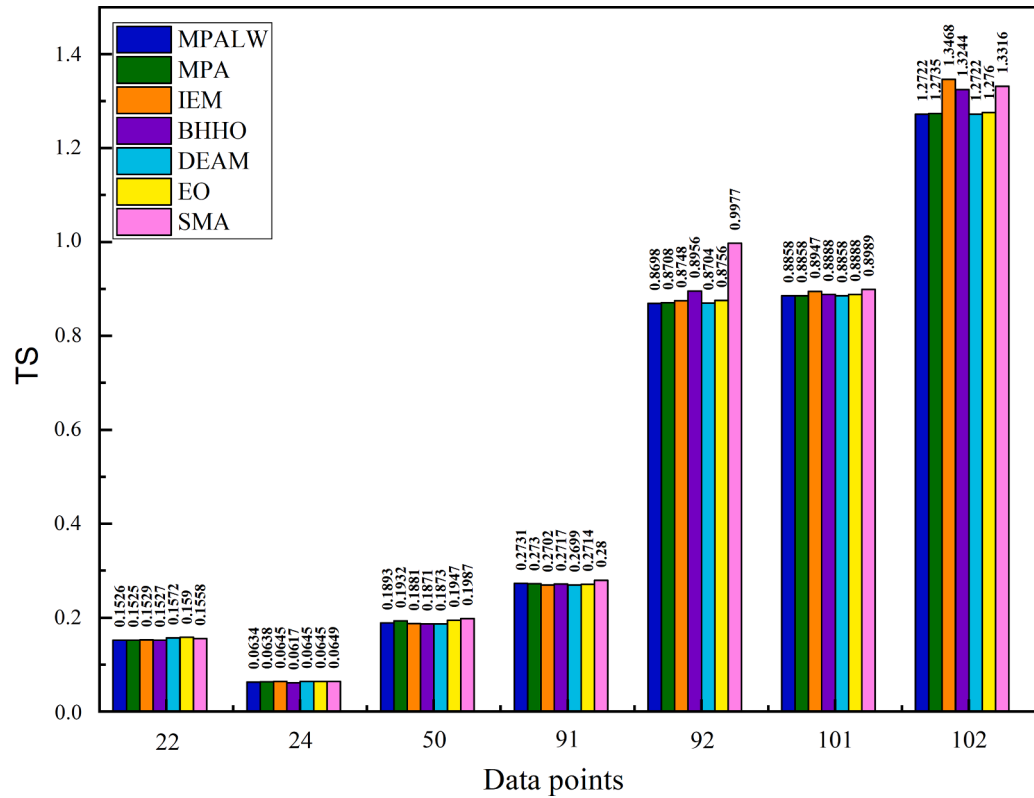


Fig. 6. TS values of the MPALW and other methods for the SD PV model under seven environmental conditions.

same level of accuracy, except for the IEM, BHHO, and SMA methods were registered worst RMSE values. It can be note that MPALW has better accuracy among other models, particularly in high-voltage regions ended by dark red color.

Further comparison analyses are rendered using RMSE and test statistical (TS) criteria. With respect to Fig. 6, the average TS value of the MPALW is 0.5295, followed by DEAM and MPA, where their average values are 0.5297 and 0.5304, respectively. It can be seen that the worst

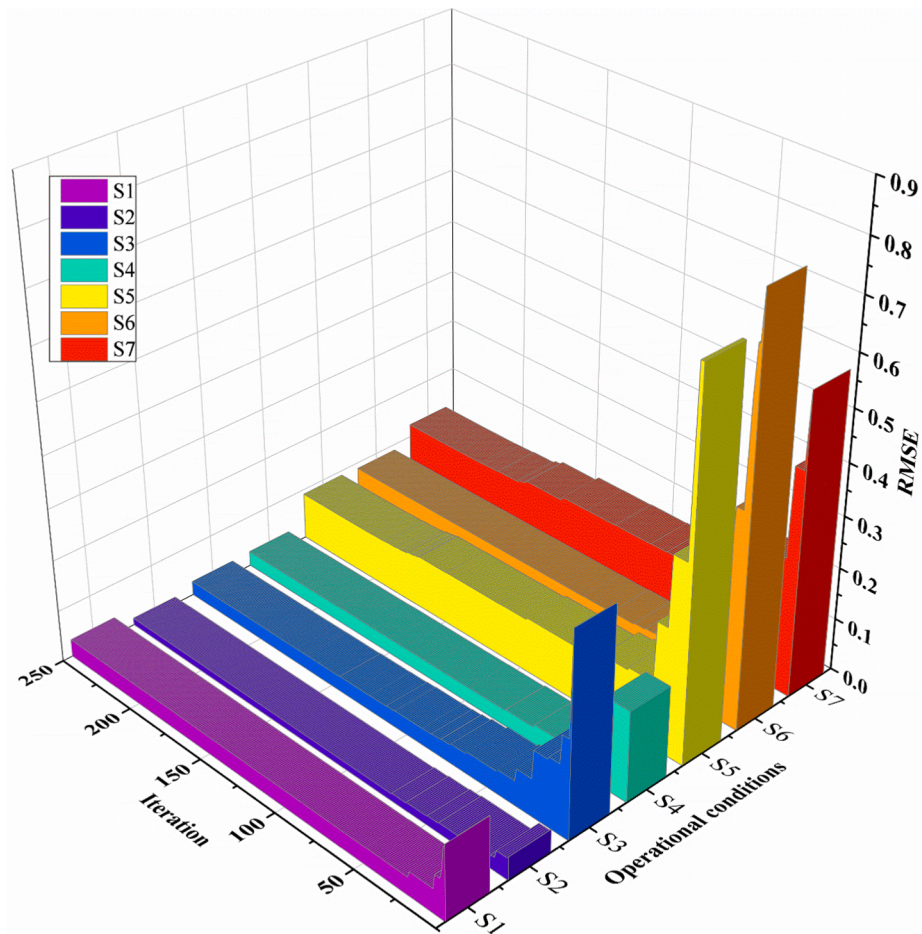


Fig. 7. Development of the RMSE values of the MPALW for the SD PV model at the seven weather conditions.

Table 6

Extracted parameters of the MPALW algorithm and other algorithms for the SD PV model.

Parameters	Method	S_1	S_2	S_3	S_4	S_5	S_6	S_7
d_1	MPALW	1.2070	1.6797	2.0000	1.9999	1.4128	1.4101	1.4703
	MPA	1.0000	1.4217	1.0416	1.8123	1.7982	1.4185	1.3839
	IEM	1.8889	1.2633	1.9030	1.9399	1.3444	1.3280	1.4078
	BHHO	1.3151	1.4137	1.1354	1.3400	1.8838	1.2407	1.5783
	DEIM	1.4037	1.8701	1.4291	1.3559	1.7652	1.4267	1.4119
	EO	1.7179	1.5543	1.9996	1.9427	1.9697	1.7606	1.6975
	SMA	1.0010	1.4993	1.1892	1.0416	1.1333	1.3493	1.3627
d_2	MPALW	1.0000	1.3895	1.1265	1.3024	1.4023	1.4215	1.5614
	MPA	1.5902	1.9219	1.4439	1.2741	1.3051	1.4228	1.4239
	IEM	1.1689	1.5504	1.1021	1.3345	1.4552	1.3775	1.4350
	BHHO	1.7059	1.4193	1.4747	1.7536	1.3859	1.9385	1.3963
	DEIM	1.7463	1.4212	1.1967	1.3554	1.3621	1.4200	1.5144
	EO	1.3838	1.5058	1.3109	1.3554	1.3263	1.3469	1.3810
	SMA	1.0000	1.8401	1.0080	1.5921	1.1267	1.0002	1.1759
I_{o1}	MPALW	1.09E-12	4.55E-06	6.40E-06	2.03E-07	3.08E-06	2.42E-06	9.99E-06
	MPA	1.54E-08	5.09E-06	9.37E-08	9.99E-06	6.51E-06	9.91E-06	3.91E-06
	IEM	7.46E-06	9.74E-07	2.54E-06	8.48E-06	5.06E-06	7.75E-06	8.44E-06
	BHHO	1.28E-06	2.51E-06	4.07E-07	4.54E-06	1.00E-05	3.17E-06	1.00E-05
	DEIM	2.93E-06	7.20E-06	2.90E-07	2.38E-06	1.74E-07	9.99E-06	9.89E-06
	EO	4.34E-09	2.65E-06	7.57E-09	9.98E-09	4.24E-07	4.81E-06	7.98E-06
	SMA	1.98E-08	1.00E-05	9.88E-07	7.62E-08	5.43E-07	1.00E-05	8.64E-06
I_{o2}	MPALW	1.94E-08	3.28E-06	4.05E-07	3.16E-06	2.68E-06	9.99E-06	8.98E-06
	MPA	3.04E-06	4.98E-06	3.30E-06	2.18E-06	4.45E-06	9.60E-06	9.88E-06
	IEM	2.28E-07	2.22E-06	3.05E-07	4.39E-06	5.34E-06	5.31E-07	6.44E-06
	BHHO	1.47E-06	2.51E-06	3.07E-06	4.38E-06	1.00E-05	3.50E-06	1.00E-05
	DEIM	2.92E-06	4.94E-06	1.05E-06	3.19E-06	8.21E-06	9.99E-06	9.97E-06
	EO	2.65E-06	8.68E-06	3.86E-06	5.57E-06	5.65E-06	9.52E-06	9.71E-06
	SMA	1.00E-12	3.26E-07	2.02E-10	5.38E-06	7.29E-09	1.00E-12	1.00E-12
I_{ph}	MPALW	0.8404	0.9258	1.9532	4.4285	5.1598	5.1816	6.4540
	MPA	0.8421	0.9239	1.9568	4.4142	5.1083	5.1726	6.4590
	IEM	0.8465	9.2206	1.9702	4.3851	4.9882	5.1493	6.4449
	BHHO	0.8541	0.9337	1.9430	4.3897	4.9849	5.1174	6.2067
	DEIM	0.8545	0.9128	1.9546	4.4070	5.1438	5.1755	6.4560
	EO	0.8511	0.9140	1.9443	4.4095	5.1323	5.1916	6.4428
	SMA	0.8353	0.9105	1.9454	4.4101	5.0872	5.1538	6.5047
R_s	MPALW	1.9317	0.3056	0.7359	0.5207	0.4824	0.3117	0.2906
	MPA	1.7859	0.2124	0.7167	0.5247	0.2771	0.1793	0.1799
	IEM	1.6215	0.3991	0.6942	0.5140	0.2741	0.2072	0.1745
	BHHO	1.4081	0.1992	0.6671	0.5204	0.2729	0.2179	0.2009
	DEIM	1.2933	0.2371	0.6464	0.5055	0.2570	0.1784	0.1725
	EO	1.3065	0.1184	0.5823	0.5054	0.2834	0.1965	0.1923
	SMA	1.9154	0.1292	0.6675	0.6099	0.3336	0.2021	0.1874
R_p	MPALW	1090.18	533.08	326.97	177.54	50.06	3417.68	38.14
	MPA	7996.72	579.09	385.54	257.15	53.71	7999.74	32.14
	IEM	7681.91	439.78	172.20	7926.18	139.41	7909.81	32.81
	BHHO	1878.75	347.48	726.71	2796.73	137.93	5183.05	132.33
	DEIM	4909.81	2698.60	362.66	426.91	45.99	3389.19	33.97
	EO	7956.07	1899.02	3029.78	370.43	50.25	290.55	35.28
	SMA	1666.17	2767.12	547.88	169.78	47.99	7785.74	27.29

values were reported by BHHO and SMA, where their average values are 0.5403 and 0.5611. Finally, the fitness function development of the MPALW method under seven environmental conditions is demonstrated in Fig. 7. According to Fig. 5, MPALW has fast coverage to the optimal solution at approximately 100 generations where the values of fitness function are 0.0338, 0.01362, 0.0321, 0.0300, 0.1032, 0.0896, and 0.1490. Significant changes occurred at S_6 and S_7 , demonstrating the powerful of using the Lambert form approach, especially at high-voltage domains. It means that the MPALW still providing global solutions in most of runs compared with other pairs.

4.2. Results on double diode PV module

The extracted parameters of the DD PV module's model using MPALW, MPA, IEM, BHHO, DEIM, EO, and SMA methods are given in Table 6. In DD PV model, two more parameters need to be optimally determined which are d_2 and I_{o2} which need more computational by the algorithms. Fig. 8 (a and b) demonstrates the I-V and P-V curves of the MPALW, MPA, IEM (H.M. Ridha et al., 2020a), BHHO (H.M. Ridha et al., 2020c), DEIM (Muhsen et al., 2015b), EO, and SMA algorithms for the

DD PV module's model under real seven weather conditions. The proposed MPALW is very close to the experimental data, followed by MPA and DEIM algorithms. The divergence can also be clearly detected by BHHO, IEM, and SMA algorithms.

For further demonstration of MPALW performance against other double diode algorithms, the results of the DD PV model are tabulated in Table 7. The minimum average RMSE value is found by MPALW, which is 0.0569, followed by MPA and DEIM. While the worst average RMSE values are registered by BHHO, which is 0.0618 followed IEM, SMA, and EO methods. In addition, the MPALW showed good performance as it had a minimum average value of 0.0046 and a high level of consistency between the experimental and computed currents 0.9947 in terms of MBE and R^2 relative to other algorithms. The second-best values of RMSE, MBE, and R^2 are 0.0577 for MPA, 0.0048 for MPA and DEIM, and 0.9945 for MPA and SMA, respectively. The worst average values of MBE and R^2 are found by BHHO, which are 0.0056 and 0.0994, respectively. It is worth mentioning that RMSE and MBE have a strong sensitivity to the noise characteristics and multi-model optimization as the real experimental data are used for this optimization problem. However, MPALW provides minimum values of RMSE and MBE and

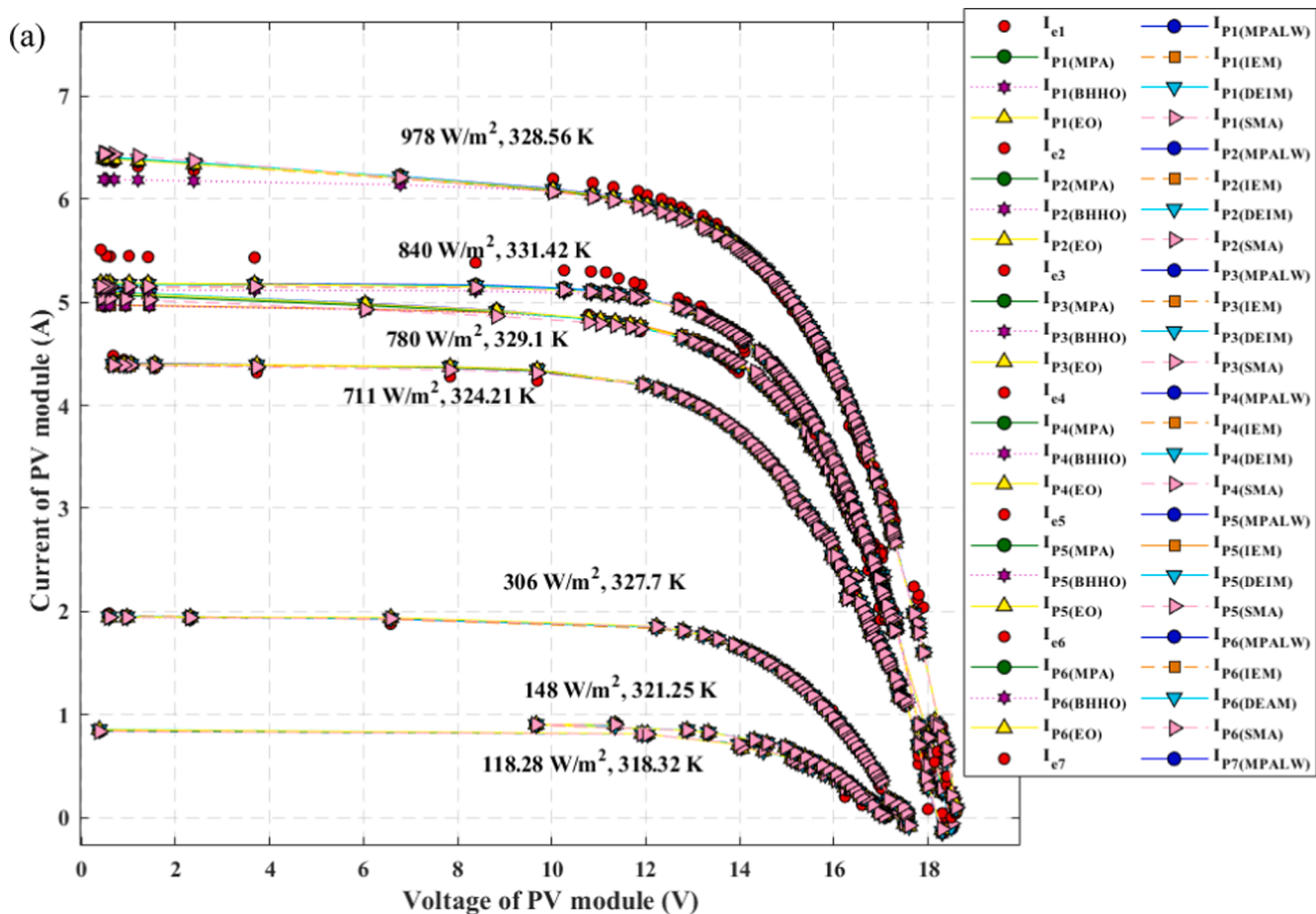


Fig. 8. Comparison between the computed and experimental data of the MPALW and other models. (a) I-V curve and (b) P-V curve.

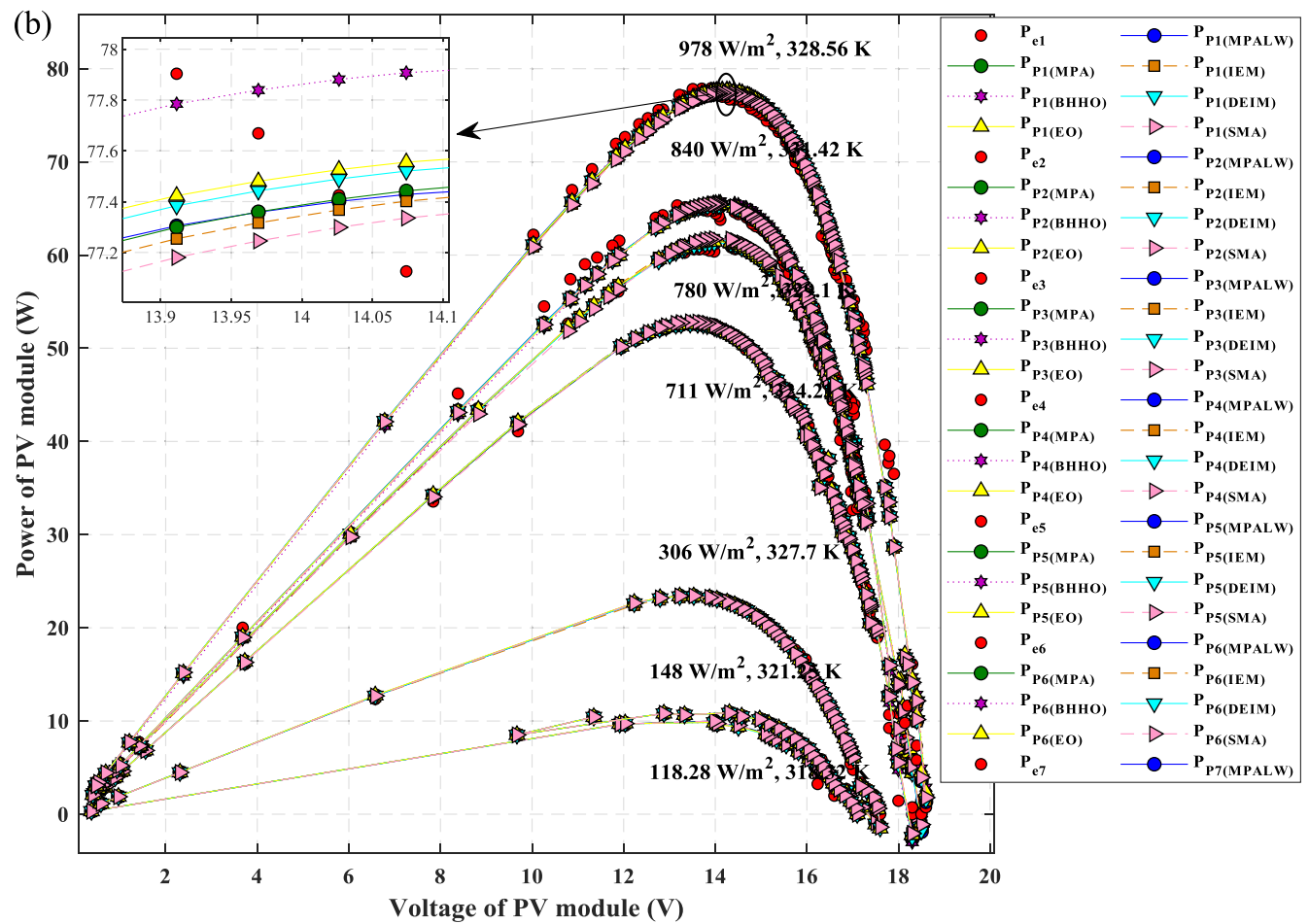


Fig. 8. (continued).

Table 7

RMSE, MBE, and R^2 of the proposed MPALW and other algorithms for the DD PV model.

Parameters	Method	S_1	S_2	S_3	S_4	S_5	S_6	S_7	Average
RMSE	MPALW	0.0329	0.0133	0.0266	0.0286	0.0914	0.0863	0.1190	0.0569
	MPA	0.0332	0.0133	0.0267	0.0287	0.0915	0.0868	0.1240	0.0577
	IEM	0.0337	0.0133	0.0262	0.0296	0.0978	0.0891	0.1237	0.0590
	BHHO	0.0342	0.0132	0.0271	0.0300	0.0986	0.0944	0.1348	0.0618
	DEIM	0.0352	0.0136	0.0270	0.0292	0.0911	0.0868	0.1226	0.0579
	EO	0.0344	0.0134	0.0282	0.0292	0.0918	0.0881	0.1250	0.0586
	SMA	0.0329	0.0134	0.0270	0.0298	0.0937	0.0885	0.1265	0.0588
MBE	MPALW	0.0010	0.0001	0.0007	0.0008	0.0083	0.0074	0.0140	0.0046
	MPA	0.0011	0.0001	0.0007	0.0008	0.0083	0.0075	0.0153	0.0048
	IEM	0.0011	0.0001	0.0006	0.0008	0.0095	0.0079	0.0153	0.0051
	BHHO	0.0011	0.0001	0.0007	0.0009	0.0097	0.0089	0.0181	0.0056
	DEIM	0.0012	0.0001	0.0007	0.0008	0.0083	0.0075	0.0150	0.0048
	EO	0.0011	0.0001	0.0008	0.0008	0.0084	0.0077	0.0156	0.0049
	SMA	0.0010	0.0001	0.0007	0.0008	0.0087	0.0078	0.0160	0.0050
R^2	MPALW	0.9835	0.9977	0.9979	0.9993	0.9948	0.9957	0.9939	0.9947
	MPA	0.9832	0.9976	0.9979	0.9993	0.9948	0.9957	0.9934	0.9945
	IEM	0.9827	0.9977	0.9979	0.9992	0.9941	0.9955	0.9934	0.9944
	BHHO	0.9822	0.9977	0.9978	0.9992	0.9940	0.9949	0.9922	0.9940
	DEIM	0.9811	0.9975	0.9978	0.9993	0.9948	0.9957	0.9935	0.9944
	EO	0.9820	0.9976	0.9976	0.9993	0.9948	0.9956	0.9933	0.9943
	SMA	0.9835	0.9976	0.9978	0.9992	0.9945	0.9955	0.9931	0.9945

high value of R^2 which can indicate that MPALW has shown well agreement with the experimental data for the most voltage-ranges. This demonstrates that MPALW is able to find accurate optimal solutions even though the dimensions of the optimization problem are expanded.

As a matter of fact, any minimization in the RMSE value is significant because it allows to determine the parameters under non-standard

weather conditions. With that in view, Fig. 9 indicates that the RMSE values for the DD PV models are less than that reported for the SD PV model. It can be easily noticed that the dark blue color, at S_2 , has minimum RMSE values. The variation of color with environmental weather conditions can then be clearly seen with the colorbar on the right side of the figure. Besides, at S_5 , the color changed from bright-

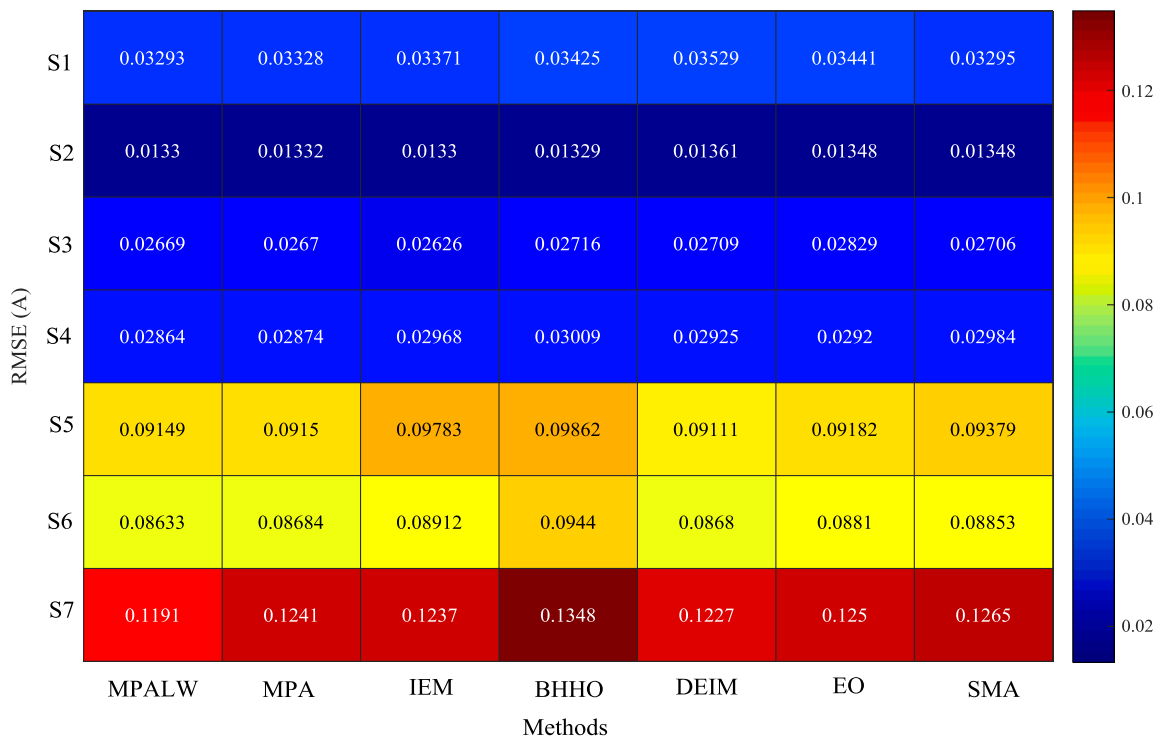


Fig. 9. Heatmap shows the relation of the RMSE values with solar radiations using several methods for the DD PV model.

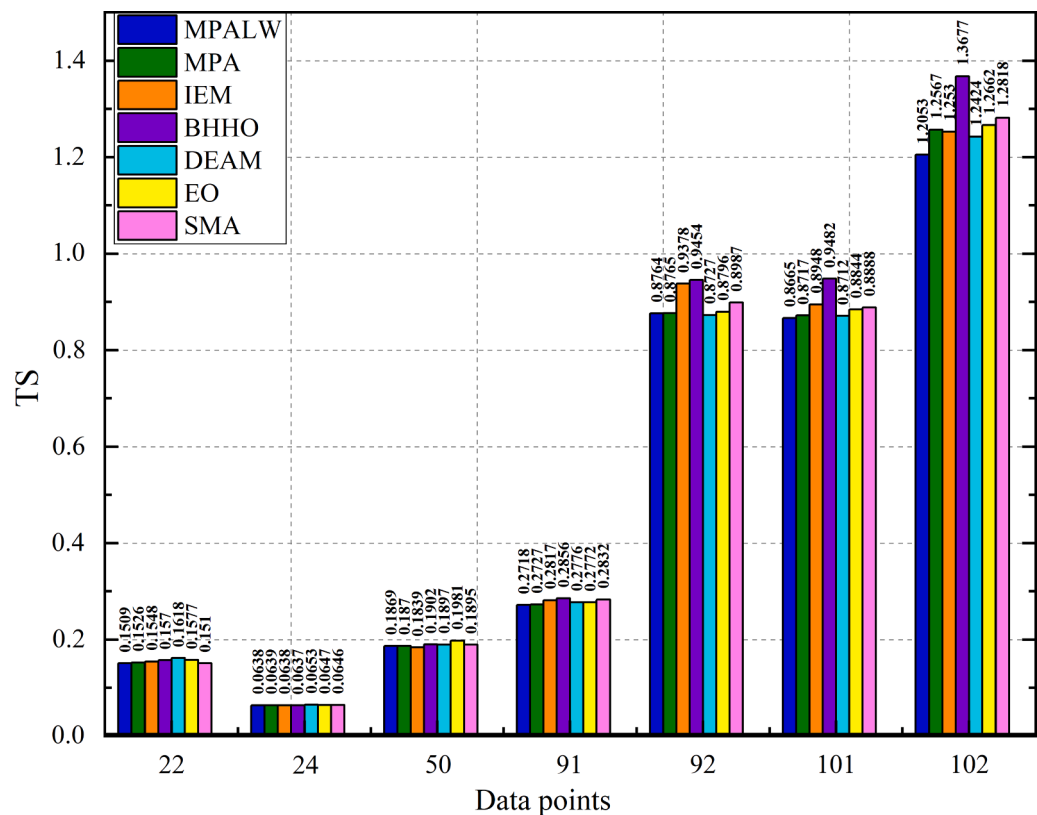


Fig. 10. TS values of the MPALW and other methods for the DD PV model under seven environmental conditions.

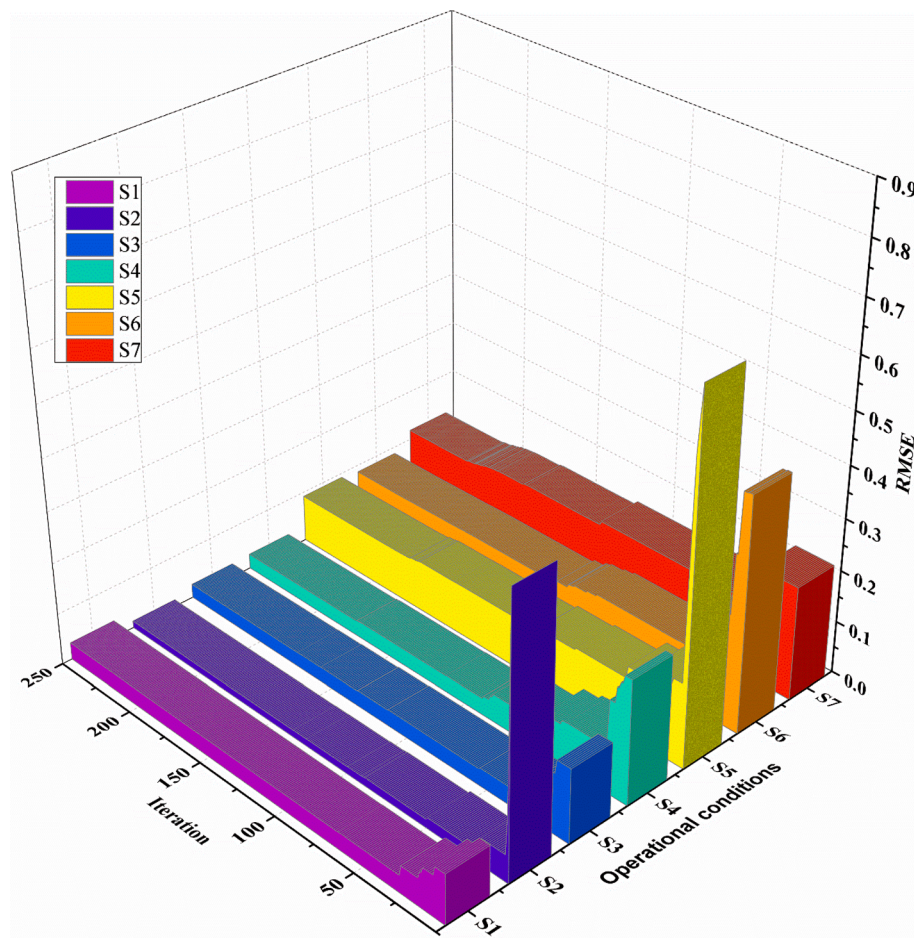


Fig. 11. Development of the RMSE values of the MPALW for the DD PV model at the seven weather conditions.

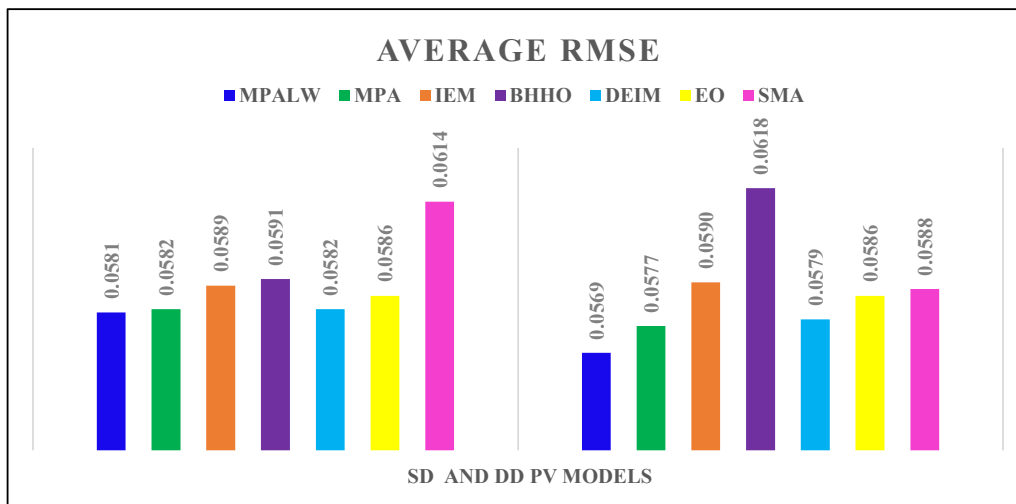


Fig. 12. Averages RMSE values for the SD and DD PV models based on MPALW and other methods.

yellow to dark-orange which denotes the small RMSE values registered by MPALW, DEIM, and MPA methods to the large RMSE values for the EO, SMA, IEM, and BHHO methods, respectively. On contrarily, the best RMSE values were recorded by MPALW for the S6 and S7 followed by DEIM methods.

For further analysis, Fig. 10 displays the TS values of the MPALW and other algorithms for the DD PV module's model. MPALW has shown dominance over other algorithms where the average TS value is 0.5174, followed by DEIM and MPA with average values of 0.5258 and 0.5259, respectively. While, the worst average TS values 0.5654, 0.5385,

0.5368, and 0.5326 for BHHO, IEM, SMA, and EO, respectively. Finally, the RMSE development of the MPALW method under seven environmental conditions for the DD PV model is shown in Fig. 11. The RMSE values of the MPALW at 100 generations are 0.0330, 0.0152, 0.0319, 0.0324, 0.0991, 0.1054, and 0.1453 for $S_1 - S_7$. It is remarked that the MPALW has faster converge as it has ability to obtain minimum value in around 100 iterations.

Based on the above findings, it can be observed that the DD PV model is more reliable than SD PV model which is promising to be applied for real-world applications (Hussein Mohammed Ridha et al., 2020a). Moreover, the formulation of the fitness function based on Lambert W function has fast convergence to the optimal solutions and can effectively solve high-nonlinearity and multi-model optimization problems (Yousri et al., 2020). To end this, a comparison of the average RMSE values for SD and DD PV models based on the utilized algorithms is depicted in Fig. 12. Note that providing a robust algorithm based on reliable objective function is main principle. Therefore, it is obvious that MPALW has minimal RMSE values in both models. However, the MPALW takes longer execution time compared with MPA based on NR method.

Wolpert et al. (Wolpert and Macready, 1997) stated that based on No Free Lunch (NFL) theorem, there is no specific method can provide a better solution than other methods for all the optimization problems. According to NFL, the authors of (Faramarzi et al., 2020) have developed the hybridized MPA method to guarantee global solutions, considering several techniques and strategies during the optimization. Various foraging strategies have substantially inspired MPA in the biological interaction between the predators and prey. Thus, the LF and Brownian distributions were designed not only to have a systematic explorer-exploiter tendency effectively, but also to significantly improve the search ability in each execution. These allowed this algorithm to accurately estimate the global optima of the optimization problems considered in this study.

5. Conclusion and future directions

The optimum simulation and proper design of the PV system needs to determine the parameters of the PV model accurately. This research paper presents the MPALW approach to precise and successful extraction of parameters of the SD and DD PV models based on actual experimental data of the PV module. To validate and analyze the performance of the MPALW, the findings obtained from MPALW are compared with state-of-the-art algorithms using multiple statistical criteria. The findings of the MPALW demonstrated a strong resemblance to experimental data and surpassed other algorithms in terms of accuracy and reliability.

For future work direction, the proposed MPALW can be improved by enhancing time scheduling strategy and exploitation ability by combining it with another technique. Furthermore, develop the Newton Raphson method to increase the accuracy of the PV models.

Declaration of Competing Interest

The authors declare that they have no known competing financial interests or personal relationships that could have appeared to influence the work reported in this paper.

Acknowledgement

The authors would like to thank Prof. Seyedali. Mirjalili for providing the MATLAB codes of the MPA and EO algorithms and for improving the quality of the manuscript.

References

- Abbassi, A., Abbassi, R., Heidari, A.A., Oliva, D., Chen, H., Habib, A., Jemli, M., Wang, M., 2020. Parameters identification of photovoltaic cell models using enhanced exploratory salp chains-based approach. Energy 117333. <https://doi.org/10.1016/j.energy.2020.117333>.
- Abbassi, A., Gammoudi, R., Ali Dami, M., Hasnaoui, O., Jemli, M., 2017. An improved single-diode model parameters extraction at different operating conditions with a view to modeling a photovoltaic generator: A comparative study. Sol. Energy 155, 478–489. <https://doi.org/10.1016/j.solener.2017.06.057>.
- Abbassi, R., Abbassi, A., Heidari, A.A., Mirjalili, S., 2019. An efficient salp swarm-inspired algorithm for parameters identification of photovoltaic cell models. Energy Convers. Manag. 179, 362–372. <https://doi.org/10.1016/j.enconman.2018.10.069>.
- Abbassi, R., Abbassi, A., Jemli, M., Chebbi, S., 2018. Identification of unknown parameters of solar cell models: A comprehensive overview of available approaches. Renew. Sustain. Energy Rev. 90, 453–474. <https://doi.org/10.1016/j.rser.2018.03.011>.
- Abdulrazzaq, A.K., Bognár, G., Plesz, B., 2020. Evaluation of different methods for solar cells/modules parameters extraction. Sol. Energy 196, 183–195. <https://doi.org/10.1016/j.solener.2019.12.010>.
- Alam, D.F., Yousri, D.A., Eteiba, M.B., 2015. Flower Pollination Algorithm based solar PV parameter estimation. Energy Convers. Manag. 101, 410–422. <https://doi.org/10.1016/j.enconman.2015.05.074>.
- Ali, E.E., El-Hameed, M.A., El-Fergany, A.A., El-Arini, M.M., 2016. Parameter extraction of photovoltaic generating units using multi-verse optimizer. Sustain. Energy Technol. Assessments 17, 68–76. <https://doi.org/10.1016/j.seta.2016.08.004>.
- Askarzadeh, A., Dos Santos Coelho, L., 2015. Determination of photovoltaic modules parameters at different operating conditions using a novel bird mating optimizer approach. Energy Convers. Manag. 89, 608–614. <https://doi.org/10.1016/j.enconman.2014.10.025>.
- Askarzadeh, A., Rezazadeh, A., 2012. Parameter identification for solar cell models using harmony search-based algorithms. Sol. Energy 86, 3241–3249. <https://doi.org/10.1016/j.solener.2012.08.018>.
- Bai, J., Liu, S., Hao, Y., Zhang, Z., Jiang, M., Zhang, Y., 2014. Development of a new compound method to extract the five parameters of PV modules. Energy Convers. Manag. 79, 294–303. <https://doi.org/10.1016/j.enconman.2013.12.041>.
- Batzelis, E.I., Papathanassiou, S.A., 2016. A method for the analytical extraction of the single-diode PV model parameters. IEEE Trans. Sustain. Energy 7, 504–512. <https://doi.org/10.1109/TSTE.2015.2503435>.
- Blaifi, S. ali, Moulahoum, S., Taghezouti, B., Saim, A., 2019. An enhanced dynamic modeling of PV module using Levenberg-Marquardt algorithm. Renew. Energy 135, 745–760. <https://doi.org/10.1016/j.renene.2018.12.054>.
- Çalasan, M., Abdel Aleem, S.H.E., Zobaa, A.F., 2020. On the root mean square error (RMSE) calculation for parameter estimation of photovoltaic models: A novel exact analytical solution based on Lambert W function, 112716 Energy Convers. Manag. 210. <https://doi.org/10.1016/j.enconman.2020.112716>.
- Chen, X., Xu, B., Mei, C., Ding, Y., Li, K., 2018a. Teaching–learning–based artificial bee colony for solar photovoltaic parameter estimation. Appl. Energy 212, 1578–1588. <https://doi.org/10.1016/j.apenergy.2017.12.115>.
- Chen, X., Yu, K., Du, W., Zhao, W., Liu, G., 2016. Parameters identification of solar cell models using generalized oppositional teaching learning based optimization. Energy 99, 170–180. <https://doi.org/10.1016/j.energy.2016.01.052>.
- Chen, X., Yue, H., Yu, K., 2019a. Perturbed stochastic fractal search for solar PV parameter estimation, 116247 Energy 189. <https://doi.org/10.1016/j.energy.2019.116247>.
- Chen, Y., Sun, Y., Meng, Z., 2018b. An improved explicit double-diode model of solar cells: Fitness verification and parameter extraction. Energy Convers. Manag. 169, 345–358. <https://doi.org/10.1016/j.enconman.2018.05.035>.
- Chen, Z., Chen, Y., Wu, L., Cheng, S., Lin, P., You, L., 2019b. Accurate modeling of photovoltaic modules using a 1-D deep residual network based on I-V characteristics. Energy Convers. Manag. 186, 168–187. <https://doi.org/10.1016/j.enconman.2019.02.032>.
- Chin, V.J., Salam, Z., 2019a. A new three-point-based approach for the parameter extraction of photovoltaic cells. Appl. Energy 237, 519–533. <https://doi.org/10.1016/j.apenergy.2019.01.009>.
- Chin, V.J., Salam, Z., 2019b. Coyote optimization algorithm for the parameter extraction of photovoltaic cells. Sol. Energy 194, 656–670. <https://doi.org/10.1016/j.solener.2019.10.093>.
- Chin, V.J., Salam, Z., Ishaque, K., 2017. An Accurate and fast computational algorithm for the two-diode model of PV module based on a hybrid method. IEEE Trans. Ind. Electron. 64, 6212–6222. <https://doi.org/10.1109/TIE.2017.2682023>.
- Dehghanzadeh, A., Farahani, G., Maboodi, M., 2017. A novel approximate explicit double-diode model of solar cells for use in simulation studies. Renew. Energy 103, 468–477. <https://doi.org/10.1016/j.renene.2016.11.051>.
- Dkhichi, F., Ouakrifi, B., Fakkari, A., Belbounaguia, N., 2014. Parameter identification of solar cell model using Levenberg-Marquardt algorithm combined with simulated annealing. Sol. Energy 110, 781–788. <https://doi.org/10.1016/j.solener.2014.09.033>.
- Easwarakhanth, T., Bottin, J., Bouhouc, I., Boutrit, C., 1986. Nonlinear Minimization Algorithm for Determining the Solar Cell Parameters with Microcomputers. Int. J. Sol. Energy 4, 1–12. <https://doi.org/10.1080/01425918608909835>.
- Einstein, A., 1956. Investigations on the Theory Brownian Movement.
- Faramarzi, A., Heidarnejad, M., Mirjalili, S., Gandomi, A.H., 2020. Marine predators algorithm: a nature-inspired metaheuristic. Expert Syst. Appl. 113377 <https://doi.org/10.1016/j.eswa.2020.113377>.
- Faramarzi, A., Heidarnejad, M., Stephens, B., Mirjalili, S., 2019. Equilibrium optimizer: A novel optimization algorithm. Knowledge-Based Syst. <https://doi.org/10.1016/j.knosys.2019.105190>.

- Fathy, A., Elaziz, M.A., Sayed, E.T., Olabi, A.G., Rezk, H., 2019. Optimal parameter identification of triple-junction photovoltaic panel based on enhanced moth search algorithm, 116025 Energy 188. <https://doi.org/10.1016/j.energy.2019.116025>.
- Fébba, D.M., Bortoni, E.C., Oliveira, A.F., Rubinger, R.M., 2020. The effects of noises on metaheuristic algorithms applied to the PV parameter extraction problem. Sol. Energy 201, 420–436. <https://doi.org/10.1016/j.solener.2020.02.093>.
- Filmalter, J.D., Dagorn, L., Cowley, P.D., Taquet, M., 2011. First descriptions of the behavior of silky sharks, *Carcharhinus falciformis*, around drifting fish aggregating devices in the Indian Ocean. Bull. Mar. Sci. 87, 325–337. <https://doi.org/10.5343/bms.2010.1057>.
- Gao, X., Cui, Y., Hu, J., Xu, G., Wang, Z., Qu, J., Wang, H., 2018. Parameter extraction of solar cell models using improved shuffled complex evolution algorithm. Energy Convers. Manag. 157, 460–479. <https://doi.org/10.1016/j.enconman.2017.12.033>.
- Gao, X., Cui, Y., Hu, J., Xu, G., Yu, Y., 2016. Lambert W-function based exact representation for double diode model of solar cells: Comparison on fitness and parameter extraction. Energy Convers. Manag. 127, 443–460. <https://doi.org/10.1016/j.enconman.2016.09.005>.
- Ghani, F., Rosengarten, G., Duke, M., Carson, J.K., 2014. The numerical calculation of single-diode solar-cell modelling parameters. Renew. Energy 72, 105–112. <https://doi.org/10.1016/j.renene.2014.06.035>.
- Gnetchejo, P.J., Essiane, S.N., Ele, P., Wamkeue, R., Wapet, D.M., Ngoffe, S.P., 2019. Enhanced vibrating particles system algorithm for parameters estimation of photovoltaic system. J. Power Energy Eng. 07, 1–26. <https://doi.org/10.4236/jpee.2019.78001>.
- Gong, W., Cai, Z., 2013. Parameter extraction of solar cell models using repaired adaptive differential evolution. Sol. Energy 94, 209–220. <https://doi.org/10.1016/j.solener.2013.05.007>.
- Guo, L., Meng, Z., Sun, Y., Wang, L., 2016. Parameter identification and sensitivity analysis of solar cell models with cat swarm optimization algorithm. Energy Convers. Manag. 108, 520–528. <https://doi.org/10.1016/j.enconman.2015.11.041>.
- Humada, A.M., Darweesh, S.Y., Mohammed, K.G., Kamil, M., Mohammed, S.F., Kasim, N. K., Tahseen, T.A., Awad, O.I., Mekhilef, S., 2020. Modeling of PV system and parameter extraction based on experimental data: Review and investigation. Sol. Energy 199, 742–760. <https://doi.org/10.1016/j.solener.2020.02.068>.
- Humphries, N.E., Queiroz, N., Dyer, J.R.M., Pade, N.G., Musyl, M.K., Schaefer, K.M., Fuller, D.W., Brunschwiler, J.M., Doyle, T.K., Houghton, J.D.R., Hays, G.C., Jones, C.S., Noble, L.R., Wearmouth, V.J., Southall, E.J., Sims, D.W., 2010. Environmental context explains Levy and Brownian movement patterns of marine predators. Nature 465, 1066–1069. <https://doi.org/10.1038/nature09116>.
- Ibrahim, I.A., Hossain, J., Duck, B.C., Fell, C.J., 2019. An adaptive wind driven optimization algorithm for extracting the parameters of a single-diode PV cell model. IEEE Trans. Sustain. Energy PP, 1–1. <https://doi.org/10.1109/tese.2019.2917513>.
- Ishaque, K., Salam, Z., Mekhilef, S., Shamsudin, A., 2012. Parameter extraction of solar photovoltaic modules using penalty-based differential evolution. Appl. Energy 99, 297–308. <https://doi.org/10.1016/j.apenergy.2012.05.017>.
- Ishaque, K., Salam, Z., Taheri, H., 2011. Simple, fast and accurate two-diode model for photovoltaic modules. Sol. Energy Mater. Sol. Cells 95, 586–594. <https://doi.org/10.1016/j.solmat.2010.09.023>.
- Jiang, L.L., Maskell, D.L., Patra, J.C., 2013. Parameter estimation of solar cells and modules using an improved adaptive differential evolution algorithm. Appl. Energy 112, 185–193. <https://doi.org/10.1016/j.apenergy.2013.06.004>.
- Kang, T., Yao, J., Jin, M., Yang, S., Duong, T., 2018. A novel improved cuckoo search algorithm for parameter estimation of photovoltaic (PV) models. Energies 11. <https://doi.org/10.3390/en11051060>.
- Kanimoorthy, G., Kumar, Harish, 2018. Modeling of solar cell under different conditions by Ant Lion Optimizer with LambertW function. Appl. Soft Comput. J. 71, 141–151. <https://doi.org/10.1016/j.asoc.2018.06.025>.
- Khanna, V., Das, B.K., Bisht, D., Vandana, Singh, P.K., 2015. A three diode model for industrial solar cells and estimation of solar cell parameters using PSO algorithm. Renew. Energy 78, 105–113. <https://doi.org/10.1016/j.renene.2014.12.072>.
- Khatib, T., 2015. A novel approach for solar radiation prediction using artificial neural networks. energy sources, Part A recover. Util. Environ. Eff. 37, 2429–2436. <https://doi.org/10.1080/15567036.2012.713080>.
- Khatib, T., Sopian, K., Kazem, H.A., 2013. Actual performance and characteristic of a grid connected photovoltaic power system in the tropics: A short term evaluation. Energy Convers. Manag. 71, 115–119. <https://doi.org/10.1016/j.enconman.2013.03.030>.
- Kler, D., Sharma, P., Banerjee, A., Rana, K.P.S., Kumar, V., 2017. PV cell and module efficient parameters estimation using evaporation rate based water cycle algorithm. Swarm Evol. Comput. 35, 93–110. <https://doi.org/10.1016/j.swevo.2017.02.005>.
- Li, S., Chen, H., Wang, M., Heidari, A.A., Mirjalili, S., 2020. Slime mould algorithm: A new method for stochastic optimization. Futur. Gener. Comput. Syst. <https://doi.org/10.1016/j.future.2020.03.055>.
- Li, S., Gong, W., Yan, X., Hu, C., Bai, D., Wang, L., 2019. Parameter estimation of photovoltaic models with memetic adaptive differential evolution. Sol. Energy 190, 465–474. <https://doi.org/10.1016/j.solener.2019.08.022>.
- Liang, J., Ge, S., Qu, B., Yu, K., Liu, F., Yang, H., Wei, P., Li, Z., 2020. Classified perturbation mutation based particle swarm optimization algorithm for parameters extraction of photovoltaic models, 112138 Energy Convers. Manag. 203. <https://doi.org/10.1016/j.enconman.2019.112138>.
- Louzazni, M., Khouya, A., Amechnoue, K., 2017. A firefly algorithm approach for determining the parameters characteristics of solar cell. Leonardo Electron. J. Pract. Technol. 235–250.
- Lun, S. xian, Wang, S., Yang, G. hong, Guo, T. ting, 2015. A new explicit double-diode modeling method based on Lambert W-function for photovoltaic arrays. Sol. Energy 116, 69–82. <https://doi.org/10.1016/j.solener.2015.03.043>.
- Lun, S.X., Du, C.J., Guo, T.T., Wang, S., Sang, J.S., Li, J.P., 2013. A new explicit i-v model of a solar cell based on taylor's series expansion. Sol. Energy 94, 221–232. <https://doi.org/10.1016/j.solener.2013.04.013>.
- Mantegna, R.N., 1994. Fast, accurate algorithm for numerical simulation of Lévy stable stochastic processes. Phys. Rev. E 49, 4677–4683. <https://doi.org/10.1103/PhysRevE.49.4677>.
- Messaoud, R. Ben, 2020. Extraction of uncertain parameters of single and double diode model of a photovoltaic panel using Salp Swarm algorithm, 107446 Meas. J. Int. Meas. Confed. 154. <https://doi.org/10.1016/j.measurement.2019.107446>.
- Muhsen, D.H., Ghazali, A.B., Khatib, T., Abed, I.A., 2015a. Extraction of photovoltaic module model's parameters using an improved hybrid differential evolution/electromagnetism-like algorithm. Sol. Energy 119, 286–297. <https://doi.org/10.1016/j.solener.2015.07.008>.
- Muhsen, D.H., Ghazali, A.B., Khatib, T., Abed, I.A., 2015b. Parameters extraction of double diode photovoltaic module's model based on hybrid evolutionary algorithm. Energy Convers. Manag. 105, 552–561. <https://doi.org/10.1016/j.enconman.2015.08.023>.
- Nassar-Eddine, I., Obbadi, A., Errami, Y., El Fajri, A., Agunaou, M., 2016. Parameter estimation of photovoltaic modules using iterative method and the Lambert W function: A comparative study. Energy Convers. Manag. 119, 37–48. <https://doi.org/10.1016/j.enconman.2016.04.030>.
- Niu, Q., Zhang, L., Li, K., 2014. A biogeography-based optimization algorithm with mutation strategies for model parameter estimation of solar and fuel cells. Energy Convers. Manag. 86, 1173–1185. <https://doi.org/10.1016/j.enconman.2014.06.026>.
- Nunes, H.G.G., Pombo, J.A.N., Bento, P.M.R., Mariano, S.J.P.S., Calado, M.R.A., 2019. Collaborative swarm intelligence to estimate PV parameters. Energy Convers. Manag. 185, 866–890. <https://doi.org/10.1016/j.enconman.2019.02.003>.
- Nunes, H.G.G., Pombo, J.A.N., Mariano, S.J.P.S., Calado, M.R.A., Felipe de Souza, J.A. M., 2018. A new high performance method for determining the parameters of PV cells and modules based on guaranteed convergence particle swarm optimization. Appl. Energy 211, 774–791. <https://doi.org/10.1016/j.apenergy.2017.11.078>.
- Oliva, D., Cuevas, E., Pajares, G., 2014. Parameter identification of solar cells using artificial bee colony optimization. Energy 72, 93–102. <https://doi.org/10.1016/j.energy.2014.05.011>.
- Oliva, D., Elaziz, M.A., Elsheikh, A.H., Ewees, A.A., 2019. A review on meta-heuristics methods for estimating parameters of solar cells, 126683 J. Power Sources 435. <https://doi.org/10.1016/j.jpowsour.2019.05.089>.
- Perera, A.T.D., Nik, V.M., Chen, D., Scartezzini, J.L., Hong, T., 2020. Quantifying the impacts of climate change and extreme climate events on energy systems. Nat. Energy 5, 150–159. <https://doi.org/10.1038/s41560-020-0558-0>.
- Qais, M.H., Hasanien, H.M., Alghuwainem, S., 2020. Transient search optimization for electrical parameters estimation of photovoltaic module based on datasheet values, 112904 Energy Convers. Manag. 214. <https://doi.org/10.1016/j.enconman.2020.112904>.
- Qais, M.H., Hasanien, H.M., Alghuwainem, S., 2019. Identification of electrical parameters for three-diode photovoltaic model using analytical and sunflower optimization algorithm. Appl. Energy 250, 109–117. <https://doi.org/10.1016/j.apenergy.2019.05.013>.
- Rezaee Jordehi, A., 2018. Enhanced leader particle swarm optimisation (ELPSO): An efficient algorithm for parameter estimation of photovoltaic (PV) cells and modules. Sol. Energy 159, 78–87. <https://doi.org/10.1016/j.solener.2017.10.063>.
- Ridha, Hussein Mohammed, Gomes, C., Hazim, H., Ahmadipour, M., 2020a. Sizing and implementing off-grid stand-alone photovoltaic/battery systems based on multi-objective optimization and techno-economic (MADE) analysis. Energy 207. <https://doi.org/10.1016/j.energy.2020.118163>.
- Ridha, H.M., Gomes, C., Hizam, H., 2020b. Estimation of photovoltaic module model's parameters using an improved electromagnetic-like algorithm. Neural Comput. Appl. <https://doi.org/10.1007/s00521-020-04714-z>.
- Ridha, H.M., Gomes, C., Hizam, H., Ahmadipour, M., Asghar Heidari, A., Chen, H., 2021. Multi-objective optimization and multi-criteria decision-making methods for optimal design of standalone photovoltaic system: A comprehensive review, 110202 Renew. Sustain. Energy Rev. 135. <https://doi.org/10.1016/j.rser.2020.110202>.
- Ridha, H.M., Gomes, C., Hizam, H., Ahmadipour, M., Muhsen, D.H., Ethaib, S., 2020c. Optimum design of a standalone solar photovoltaic system based on novel integration of iterative-PESA-II and AHP-VIKOR methods. Processes 8. <https://doi.org/10.3390/pr8030367>.
- Ridha, Hussein Mohammed, Gomes, C., Hizam, H., Mirjalili, S., 2020b. Multiple scenarios multi-objective salp swarm optimization for sizing of standalone photovoltaic system. Renew. Energy 153, 1330–1345. <https://doi.org/10.1016/j.renene.2020.02.016>.
- Ridha, Hussein Mohammed, Heidari, A.A., Wang, M., Chen, H., 2020c. Boosted mutation-based Harris hawks optimizer for parameters identification of single-diode solar cell models. Energy Convers. Manag. 209 <https://doi.org/10.1016/j.enconman.2020.112660>.
- Selam, S.I., Hasanien, H.M., El-Fergany, A.A., 2020. Parameters extraction of PEMFC's model using manta rays foraging optimizer. Int. J. Energy Res. 44, 4629–4640. <https://doi.org/10.1002/er.5244>.
- Subudhi, B., Pradhan, R., 2018. Bacterial Foraging Optimization approach to parameter extraction of a photovoltaic module. IEEE Trans. Sustain. Energy 9, 381–389. <https://doi.org/10.1109/TSTE.2017.2736060>.
- Sudhakar Babu, T., Prasanth Ram, J., Sangeetha, K., Laudani, A., Rajasekar, N., 2016. Parameter extraction of two diode solar PV model using Fireworks algorithm. Sol. Energy 140, 265–276. <https://doi.org/10.1016/j.solener.2016.10.044>.

- Tong, N.T., Pora, W., 2016. A parameter extraction technique exploiting intrinsic properties of solar cells. *Appl. Energy* 176, 104–115. <https://doi.org/10.1016/j.apenergy.2016.05.064>.
- Tossa, A.K., Soro, Y.M., Azoumah, Y., Yamegueu, D., 2014. A new approach to estimate the performance and energy productivity of photovoltaic modules in real operating conditions. *Sol. Energy* 110, 543–560. <https://doi.org/10.1016/j.solener.2014.09.043>.
- Villalva, M.G., Gazoli, J.R., Filho, E.R., 2009. Comprehensive Approach to Modeling and Simulation of Photovoltaic Arrays. *IEEE Trans. Power Electron.* 24, 1198–1208. <https://doi.org/10.1109/tpe.2009.2013862>.
- Wolpert, D.H., Macready, W.G., 1997. No free lunch theorems for optimization. *IEEE Trans. Evol. Comput.* 1, 67–82. <https://doi.org/10.1109/4235.585893>.
- Wu, L., Chen, Z., Long, C., Cheng, S., Lin, P., Chen, Y., Chen, H., 2018. Parameter extraction of photovoltaic models from measured I-V characteristics curves using a hybrid trust-region reflective algorithm. *Appl. Energy* 232, 36–53. <https://doi.org/10.1016/j.apenergy.2018.09.161>.
- Wu, Z., Yu, D., Kang, X., 2017. Parameter identification of photovoltaic cell model based on improved ant lion optimizer. *Energy Convers. Manag.* 151, 107–115. <https://doi.org/10.1016/j.enconman.2017.08.088>.
- Xu, S., Wang, Y., 2017. Parameter estimation of photovoltaic modules using a hybrid flower pollination algorithm. *Energy Convers. Manag.* 144, 53–68. <https://doi.org/10.1016/j.enconman.2017.04.042>.
- Yan, Z., Li, C., Song, Z., Xiong, L., Luo, C., 2019. An Improved Brain Storming Optimization Algorithm for Estimating Parameters of Photovoltaic Models. *IEEE Access* 7, 77629–77641. <https://doi.org/10.1109/ACCESS.2019.2922327>.
- Yang, B., Wang, J., Zhang, X., Yu, T., Yao, W., Shu, H., Zeng, F., Sun, L., 2020. Comprehensive overview of meta-heuristic algorithm applications on PV cell parameter identification, 112595 *Energy Convers. Manag.* 208. <https://doi.org/10.1016/j.enconman.2020.112595>.
- Yang, X.-S., 2010. Engineering optimisation: an introduction with metaheuristic applications. John Wiley and Sons. <https://doi.org/10.1002/9781119483151.ch2>.
- Yang, X., Gong, W., Wang, L., 2019. Comparative study on parameter extraction of photovoltaic models via differential evolution, 112113 *Energy Convers. Manag.* 201. <https://doi.org/10.1016/j.enconman.2019.112113>.
- Yousrif, D., Abd Elaziz, M., Oliva, D., Abualigah, L., Al-qaness, M.A.A., Ewees, A.A., 2020. Reliable applied objective for identifying simple and detailed photovoltaic models using modern metaheuristics: Comparative study, 113279 *Energy Convers. Manag.* 223. <https://doi.org/10.1016/j.enconman.2020.113279>.
- Yu, K., Qu, B., Yue, C., Ge, S., Chen, X., Liang, J., 2019. A performance-guided JAYA algorithm for parameters identification of photovoltaic cell and module. *Appl. Energy* 237, 241–257. <https://doi.org/10.1016/j.apenergy.2019.01.008>.
- Zhang, H., Heidari, A.A., Wang, M., Zhang, L., Chen, H., Li, C., 2020. Orthogonal Nelder-Mead moth flame method for parameters identification of photovoltaic modules. *Energy Convers. Manag.* 211 <https://doi.org/10.1016/j.enconman.2020.112764>.